

**Supporting Information for:**

**A drug-like small molecule that targets r(CCUG) repeats in myotonic dystrophy type 2 facilitates degradation by RNA quality control pathways**

Sarah Wagner-Griffin<sup>†</sup>, Masahito Abe<sup>†</sup>, Raphael I. Benhamou, Alicia J. Angelbello, Kamalakannan Vishnu, Jonathan L. Chen, Jessica L. Childs-Disney and Matthew D. Disney<sup>a,\*</sup>

<sup>a</sup>The Scripps Research Institute, Department of Chemistry, 130 Scripps Way, Jupiter, FL 33458, USA

<sup>†</sup> These authors contributed equally.

\*Author to whom correspondence is addressed; Email: [disney@scripps.edu](mailto:disney@scripps.edu)

**Table of Contents:**

- I. Supplementary Tables & Figures
- II. Synthetic Schemes
- III. Compound Characterization

I. **Supplementary Tables & Figures**

**Table S1.** Approximate IC<sub>50</sub> for the disruption of the r(CCUG)<sup>exp</sup>-MBNL1 complex by various compounds.

<b>Compound ID</b>	<b>IC<sub>50</sub> (μM)</b>	<b>Compound ID</b>	<b>IC<sub>50</sub> (μM)</b>	<b>Compound ID</b>	<b>IC<sub>50</sub> (μM)</b>
1	30	29	100	57	105
2	35	30	105	58	15
3	40	31	105	59	60
4	40	32	110	60	200
5	45	33	135	61	200
6	50	34	135	62	10
7	50	35	150	63	2
8	50	36	155	64	30
9	60	37	165	65	200
10	60	38	190	66	200
11	65	39	200	67	200
12	70	40	200	68	20
13	70	41	200	69	200
14	70	42	200	70	200
15	70	43	200	71	0.4
16	70	44	200	72	0.2
17	75	45	200	73	0.3
18	75	46	170	74	0.3
19	80	47	135	75	105
20	80	48	70	76	110
21	80	49	10	77	20
22	85	50	7	78	1
23	85	51	30	79	4
24	90	52	200	80	10
25	95	53	200	81	10
26	95	54	90	82	1
27	100	55	200		
28	100	56	200		

<b>Table S2.</b> Sequences of primers used for RT-PCR and RT-qPCR			
Gene	Forward Primer (5'-3')	Reverse Primer (5'-3')	Purpose
<i>MAP4K4</i> Exon 22a	CCTCATCCAGTGAGGAGTCG	TGGTGGGAGAAATGCTGTATGC	RT-PCR
<i>IR</i> Exon 11	CCAAAGACAGACTCTCAGAT	AACATCGCCAAGGGACCTGC	RT-PCR
<i>GAPDH</i>	AAGGTGAAGGTCGGAGTCAA	AATGAAGGGGTCATTGATGG	qPCR
<i>CNBP</i> intron 1	ATTCCAAGGTTGGTTGAAGC	AACCCAAACCAATGAAGCTG	qPCR
<i>CNBP</i> mature mRNA	AAACTGGTCATGTAGCCATCAAC	AATTGTGCATTCCCGTGCAAG	qPCR

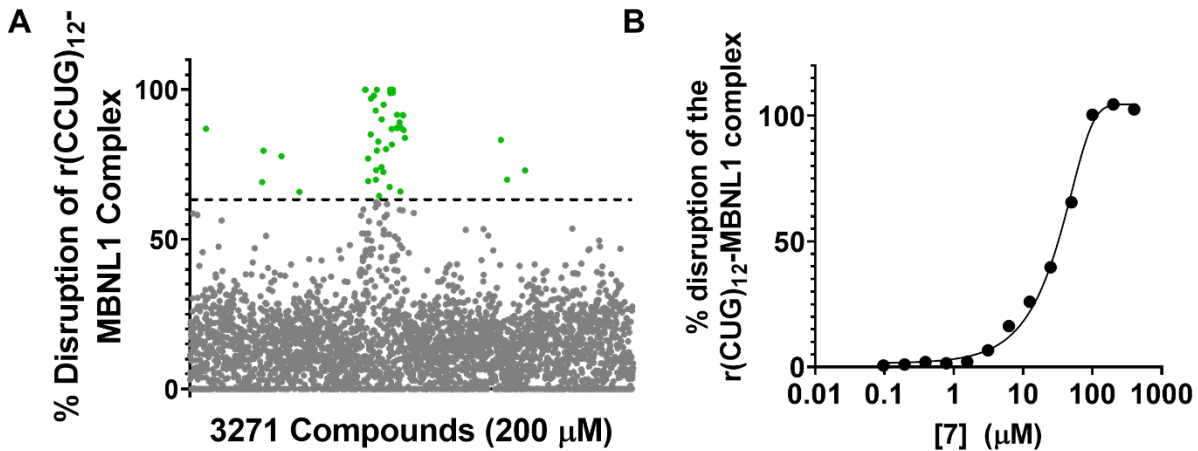


**Figure S1.** Results of a high throughput screen to identify small molecules that disrupt the  $r(\text{CCUG})_{12}$ -MBNL1 complex, a validated *in vitro* model<sup>1</sup> of the disease-causing interaction that causes DM2. (A) All 3,271 compounds in the library were screened at 200  $\mu\text{M}$ . Compounds that exhibited a percent disruption  $>3$  standard deviations from the mean ( $3\sigma$ ;  $>60\%$  disruption) are highlighted in green. (B) Representative curve of the disruption of  $r(\text{CCUG})_{12}$ -MBNL1 complex by compound 7.

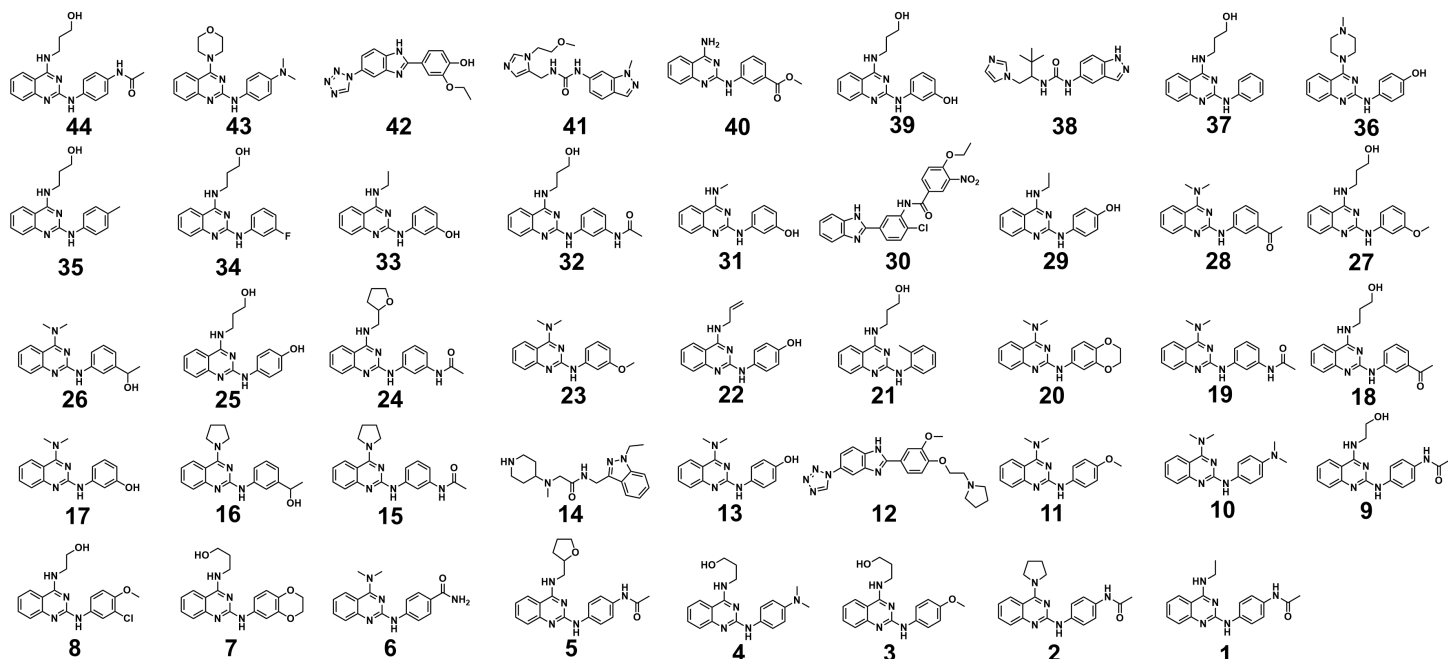
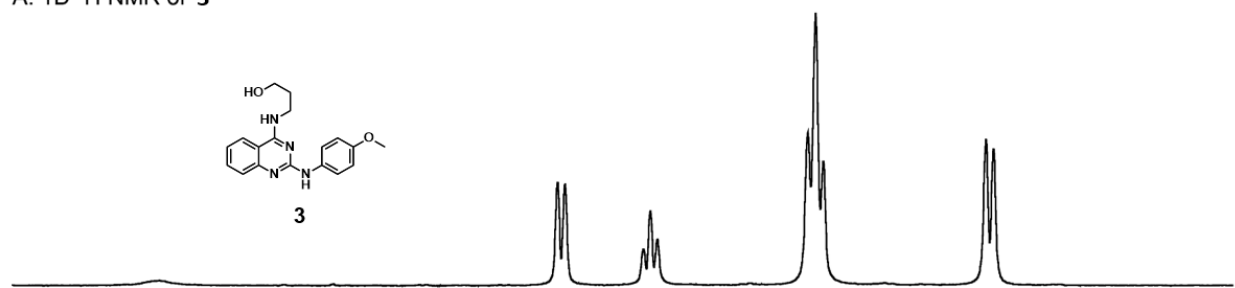


**Figure S2. Structures of compounds 1 – 44.** Structures of hit compounds from the high throughput screen of the RNA-focused library that disrupt  $r(\text{CCUG})_{12}$ -MBNL1 complex greater than 60%.

A. 1D  $^1\text{H}$  NMR of **3**



B. WaterLOGSY NMR spectra of **3**

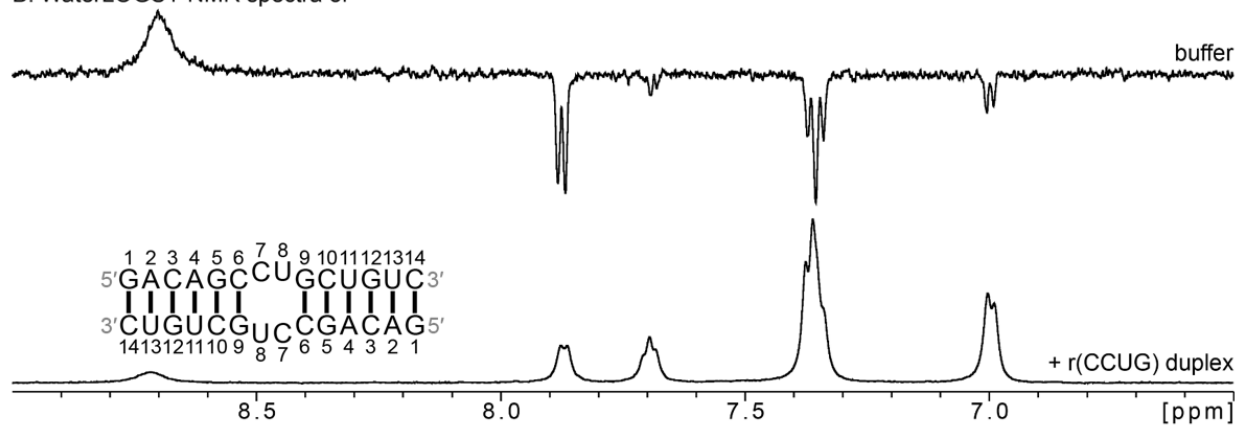
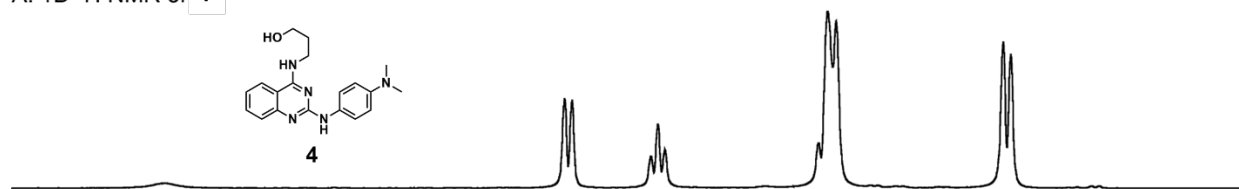
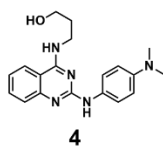


**Figure S3. WaterLOGSY NMR analysis of **3** with  $r(\text{GACAGCCUGCUGUC})_2$  duplex. (A) 1D  $^1\text{H}$  NMR of **3**. (B) WaterLOGSY NMR spectra of **3**.**

A. 1D  $^1\text{H}$  NMR of **4**



B. WaterLOGSY NMR spectra of **4**

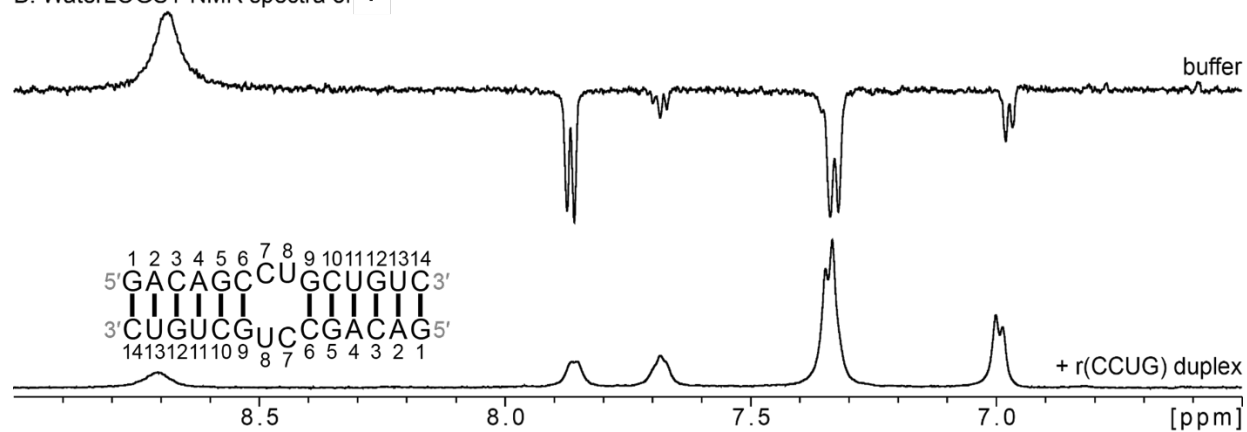
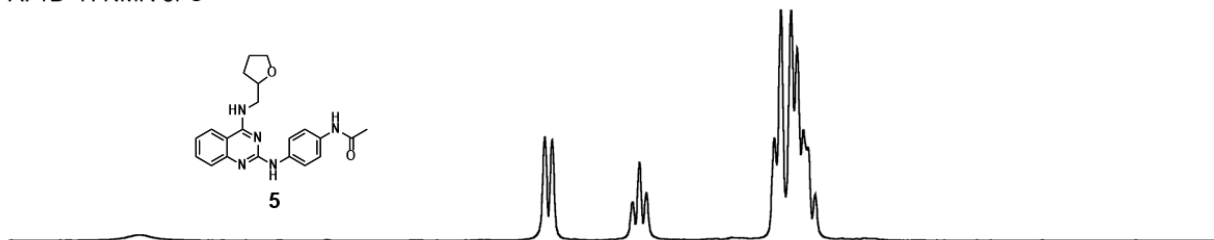


**Figure S4. WaterLOGSY NMR analysis of **4** with  $r(\text{GACAGCCUGCUGUC})_2$  duplex. (A) 1D  $^1\text{H}$  NMR of **4**. (B) WaterLOGSY NMR spectra of **4**.**

A. 1D  $^1\text{H}$  NMR of 5



B. WaterLOGSY NMR spectra of 5

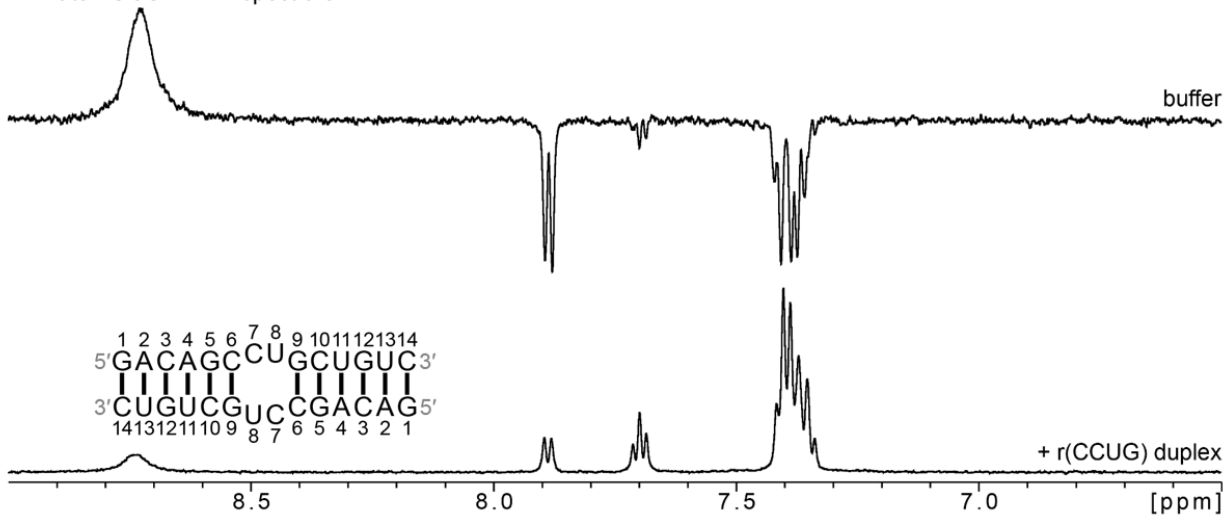
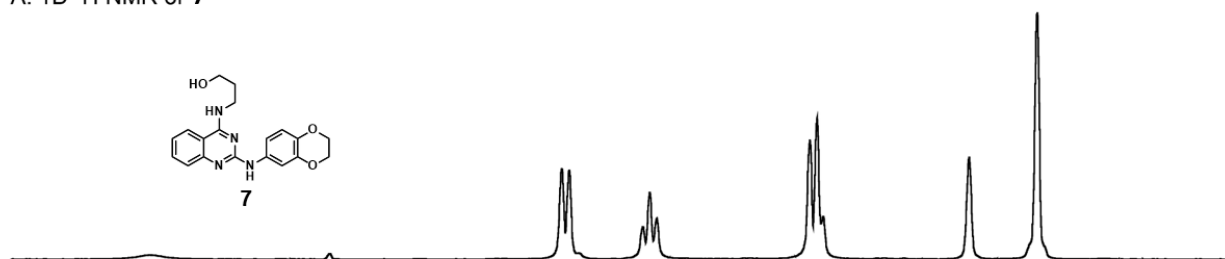


**Figure S5. WaterLOGSY NMR analysis of 5 with r(GACAGCCUGCUGUC)<sub>2</sub> duplex. (A) 1D**

**$^1\text{H}$  NMR of 5. (B) WaterLOGSY NMR spectra of 5.**

A. 1D  $^1\text{H}$  NMR of **7**



B. WaterLOGSY NMR spectra of **7**

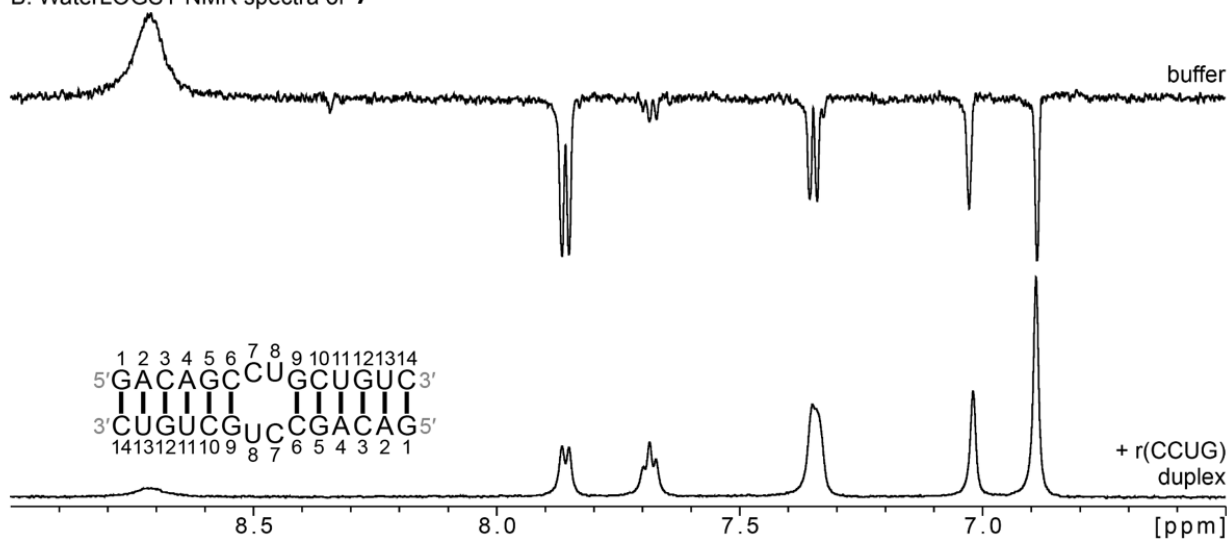


**Figure S6. WaterLOGSY NMR analysis of **7** with  $r(\text{GACAGCCUGCUGUC})_2$  duplex.** (A) 1D  $^1\text{H}$  NMR of **7**. (B) WaterLOGSY NMR spectra of **7**.

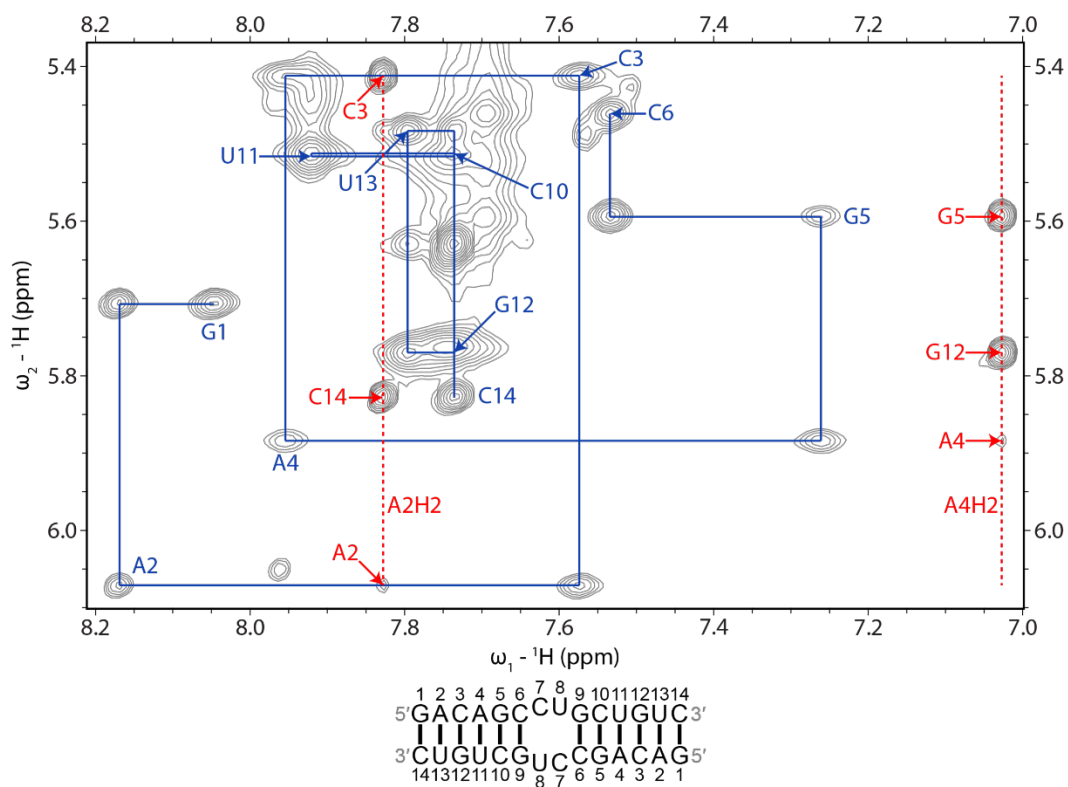


**Figure S7. 2D NOESY NMR analysis of r(GACAGCCUGCUGUC)<sub>2</sub> duplex in the absence of compound.**

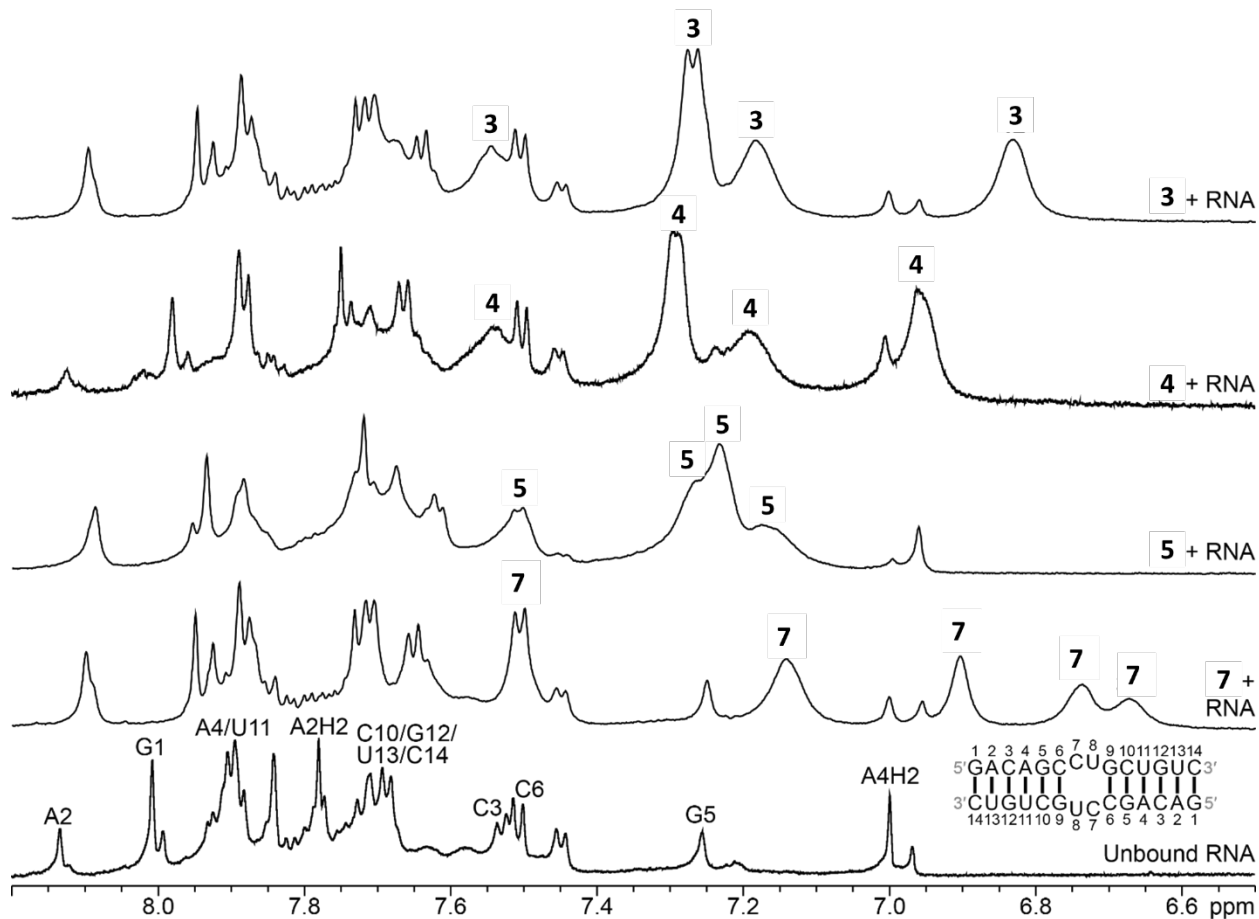


**Figure S8.** 1D NMR analysis of compounds bound to  $r(\text{GACAGCCUGCUGUC})_2$ . 1D spectra of unbound RNA (bottom) and shifts in spectra upon addition of compound.

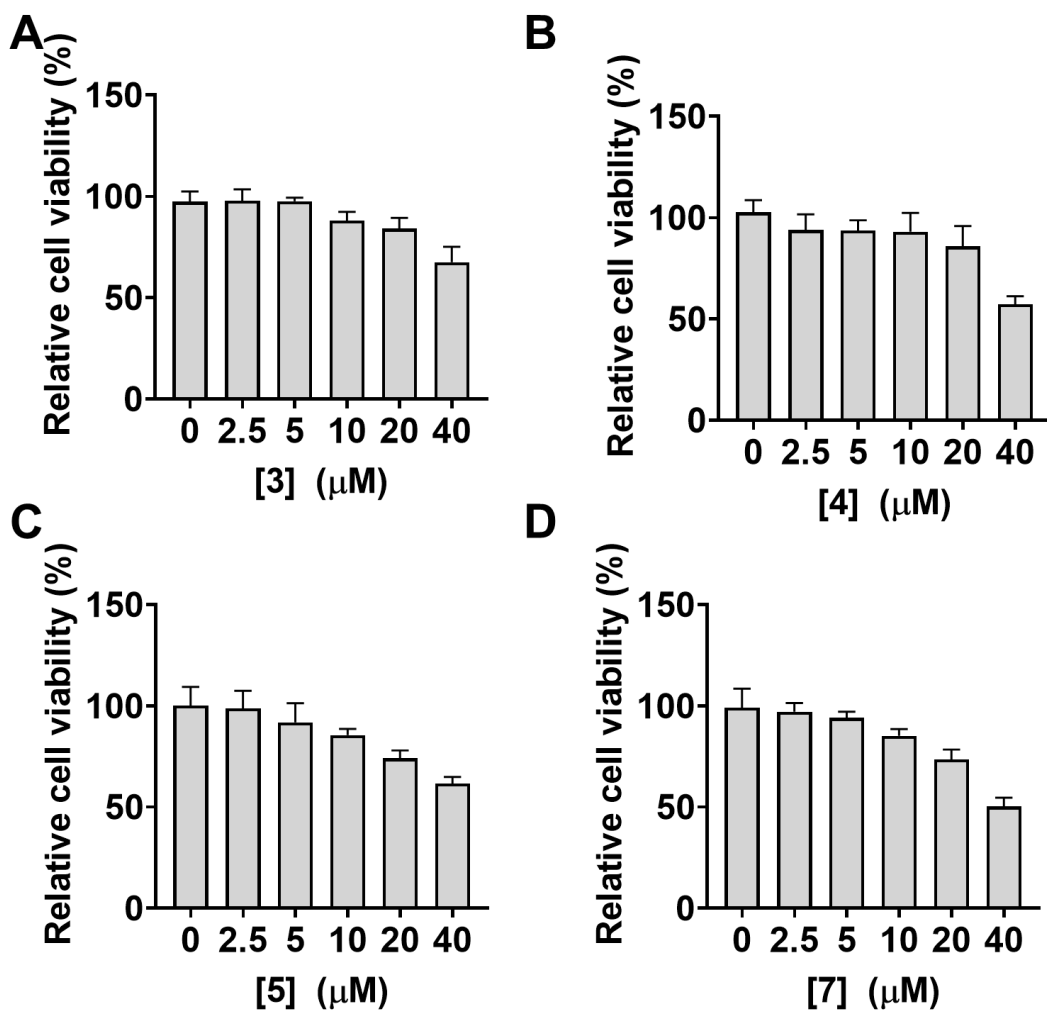
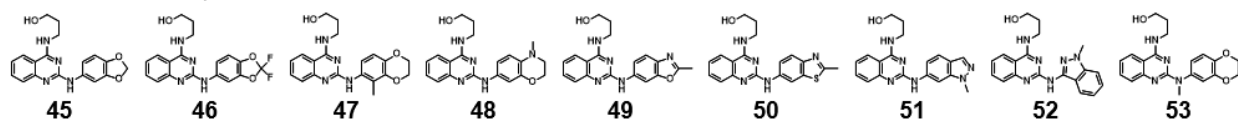
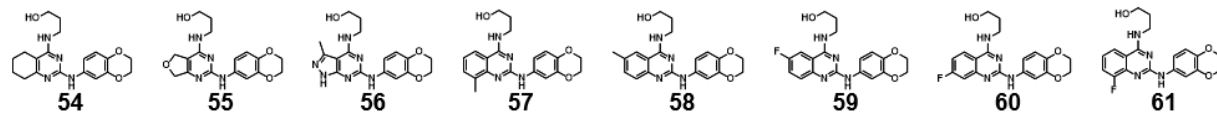


**Figure S9.** Cell viability of DM2 fibroblasts treated with 3, 4, 5, and 7, as assessed via CellTiter-Glo. Viability of cells treated with 3 (A), 4 (B), 5 (C), and 7 (D). For all panels,  $n = 5$  and error bars represent SD.

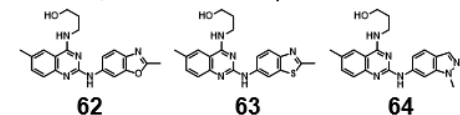
<45 - 53; Aniline replacement>



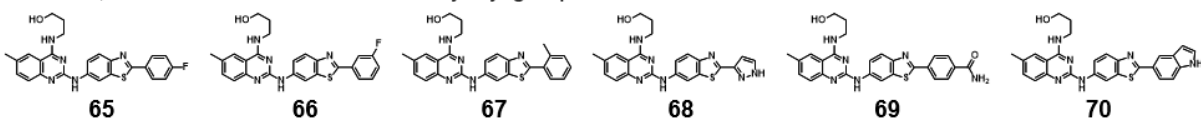
<54 – 61; Quinazoline replacement>



<62 – 64; Combination of potent scaffolds>



<65 – 70; Benzothiazole functionalization by aryl group>



<71 – 82; Benzothiazole functionalization by amine >

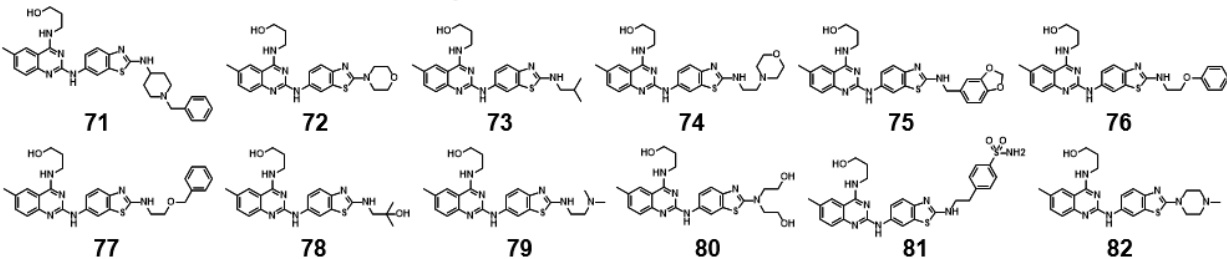
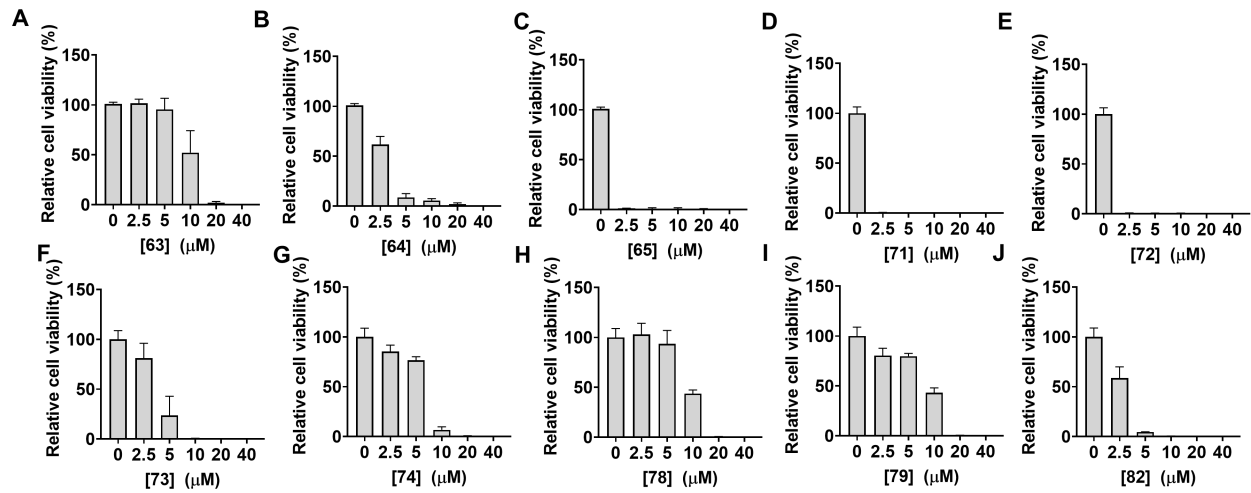
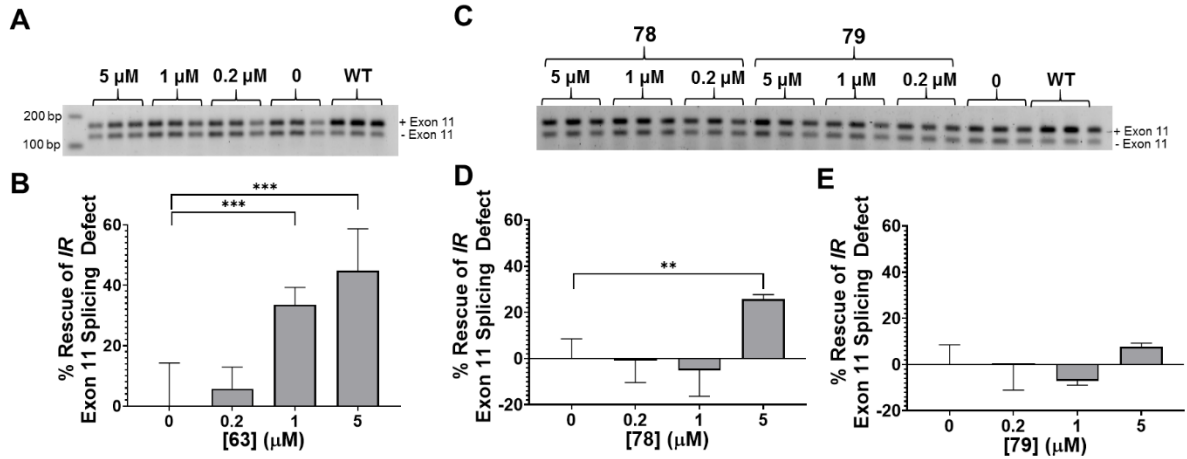


Figure S10. Structures of compounds 45 – 82.



**Figure S11. Cell viability of DM2 fibroblasts treated with lead optimized compounds, as assessed via Cell-Titer Glo.** Viability of cells treated with **63** (A), **64** (B), **65** (C), **71** (D), **72** (E), **73** (F), **74** (G), **78** (H), **79** (I), and **82** (J). For all panels, n = 5 and error bars represent SD.



**Figure S12. Cellular activity of compounds 63, 78, and 79 in DM2 fibroblasts, as assessed by rescue of *IR* exon 11 mis-splicing.** (A) Representative gel image of *IR* exon 11 splicing in DM2 fibroblasts treated with **63**. (B) Quantification of rescue of *IR* exon 11 splicing. (C) Representative gel image of *IR* exon 11 splicing in DM2 fibroblasts treated with **78** or **79**. (D) Quantification of rescue of *IR* exon 11 splicing in DM2 fibroblasts treated with **78**. (E) Quantification of rescue of *IR* exon 11 splicing in DM2 fibroblasts treated with **79**. For all panels,  $n = 3$  and error bars represent SD; \*\*  $P < 0.01$ , \*\*\*  $P < 0.001$ , as determined by one-way ANOVA relative to untreated.

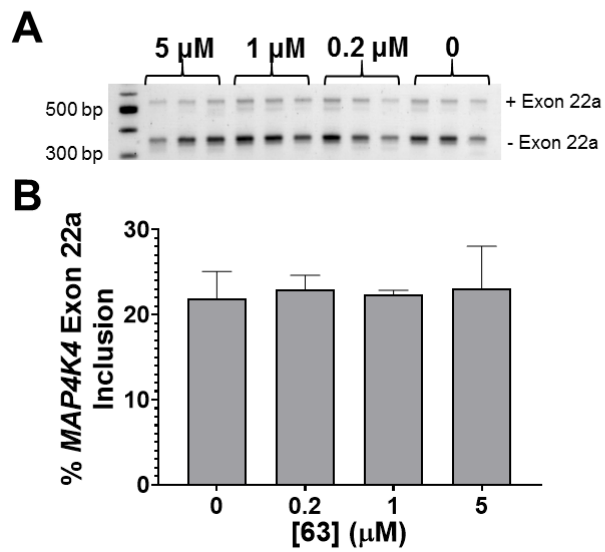


**Figure S13. Compound 63 does not affect *MAP4K4* (non-MBNL1 regulated) splicing in DM2 fibroblasts.** (A) Representative gel image of *MAP4K4* exon 22a splicing in DM2 fibroblasts treated with **63**. (B) Quantification of *MAP4K4* exon 22a inclusion; n = 3; error bars represent SD.

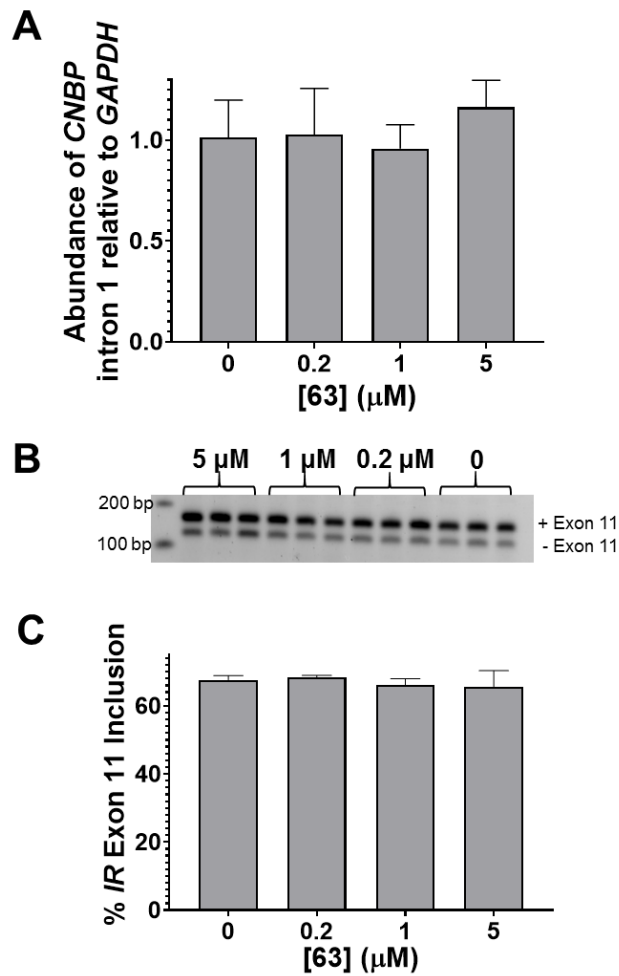
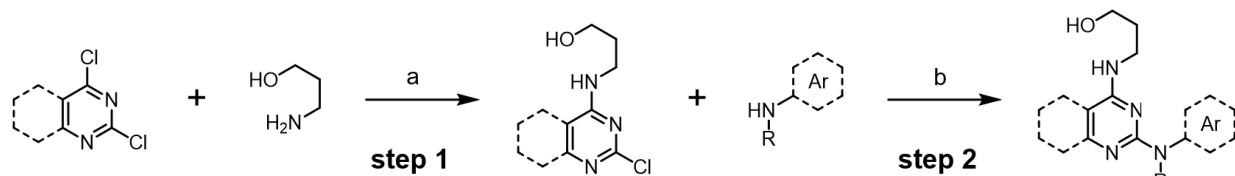
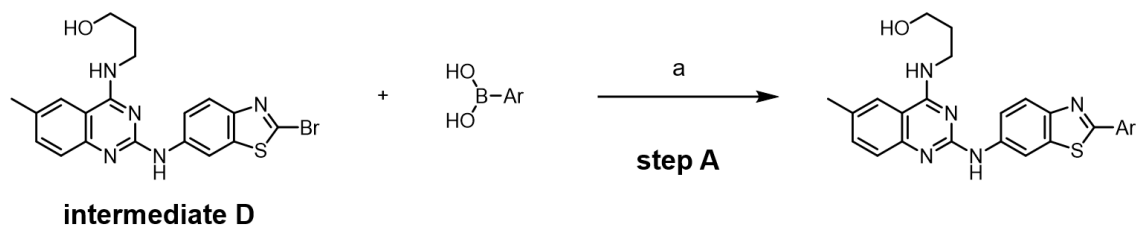


**Figure S14. Compound 63 has no effect on *CNBP* levels or *IR* exon 11 splicing in wild-type fibroblasts.** (A) Analysis of *CNBP* intron 1 levels in wild-type fibroblasts treated with **63** via RT-qPCR. (B) Representative gel image of *IR* exon 11 splicing in wild-type fibroblasts treated with **63**. (C) Quantification of *IR* exon 11 inclusion. For all panels: n = 3 and error bars represent SD.

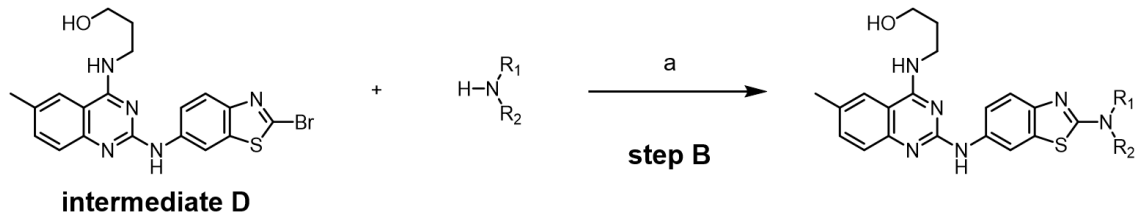
## II. Synthetic Schemes



**Scheme S1. General synthetic procedure 1 for synthesis of compounds 7, 45 – 64 and intermediate D.** Reagents and conditions; (a) 3-aminopropanol, IPA, 85 °C, 30 min, MW irradiation, (b) aniline, EtOH, 150 °C, 30-60 min, MW irradiation.



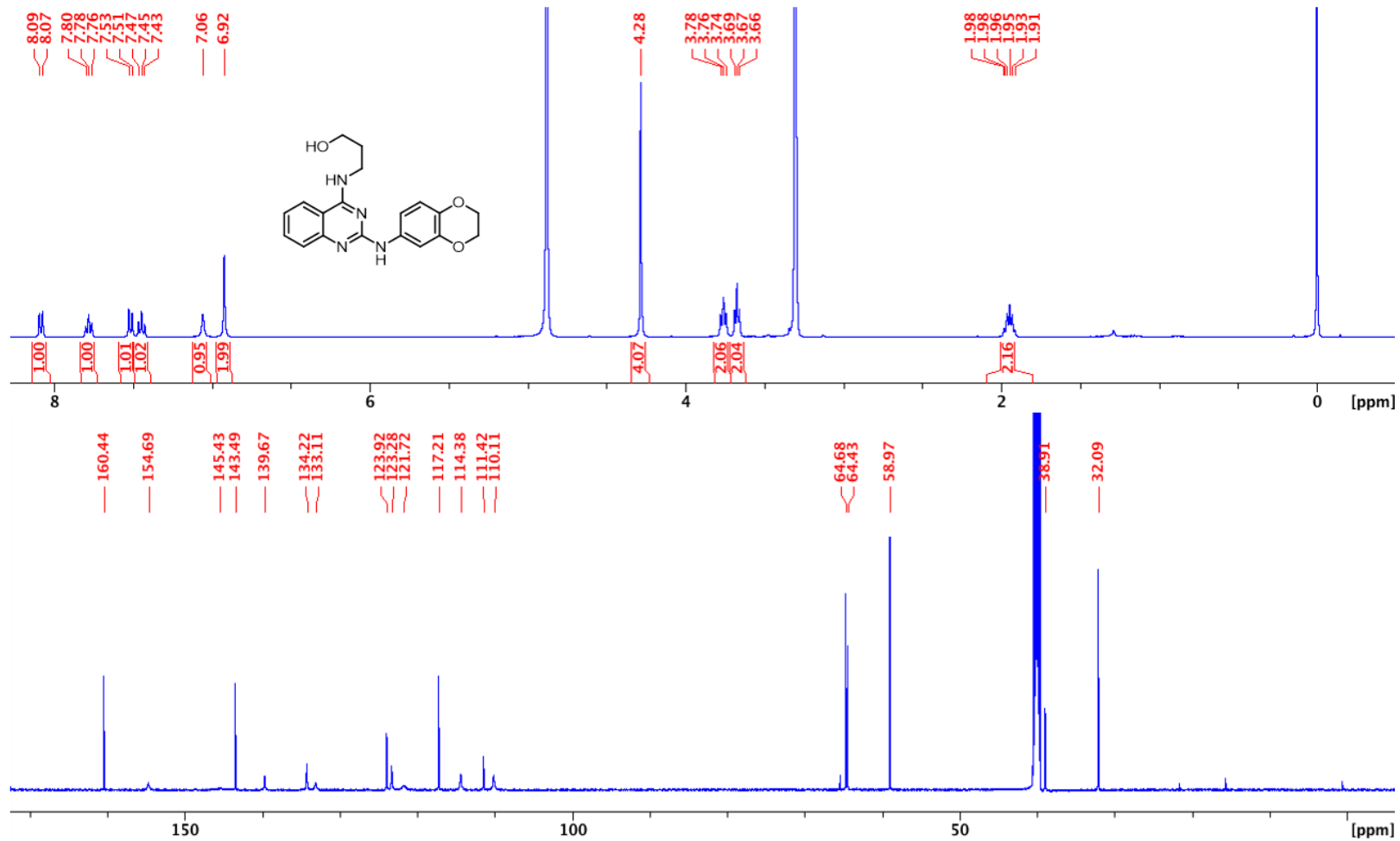
**Scheme S2. General synthetic procedure 2 for synthesis of compounds 65 – 70.** Reagents and conditions; (a) Ar-boronic acid, Pd(PPh<sub>3</sub>)<sub>4</sub>, K<sub>3</sub>PO<sub>4</sub>, dioxane/H<sub>2</sub>O (2/1), 120 °C, overnight

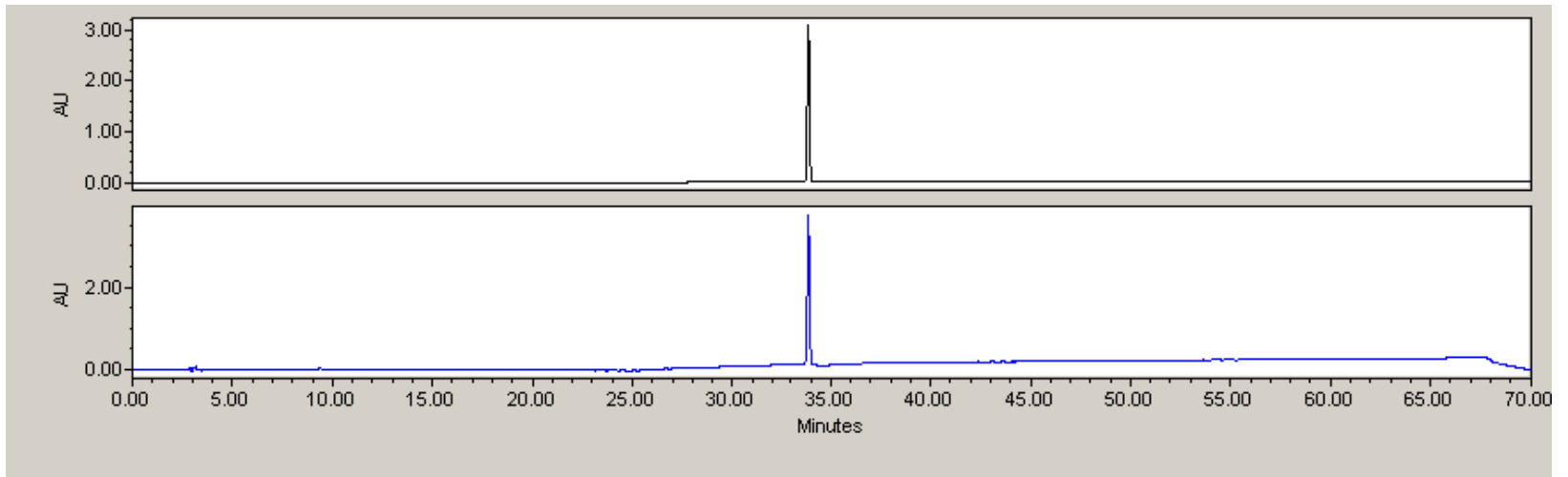


**Scheme S3. General synthetic procedure 3 for synthesis of compounds 71 – 82.** Reagents and conditions; (a) amine, DIPEA, 3-pentanol, 120 °C, overnight.

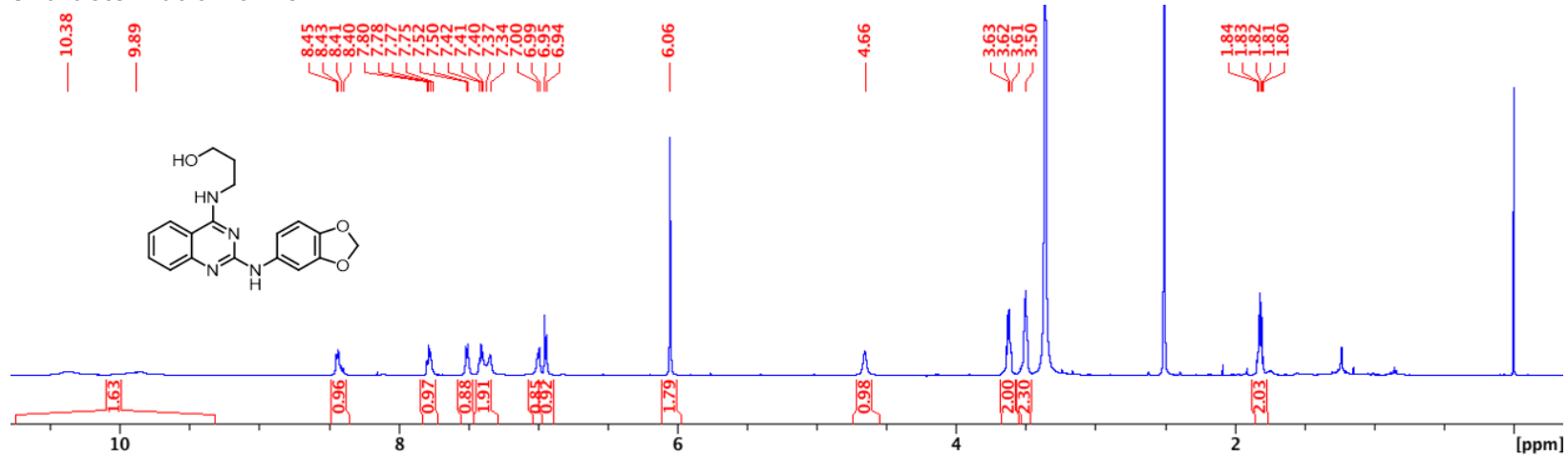
### III. Compound Characterization

#### Characterization of 7:

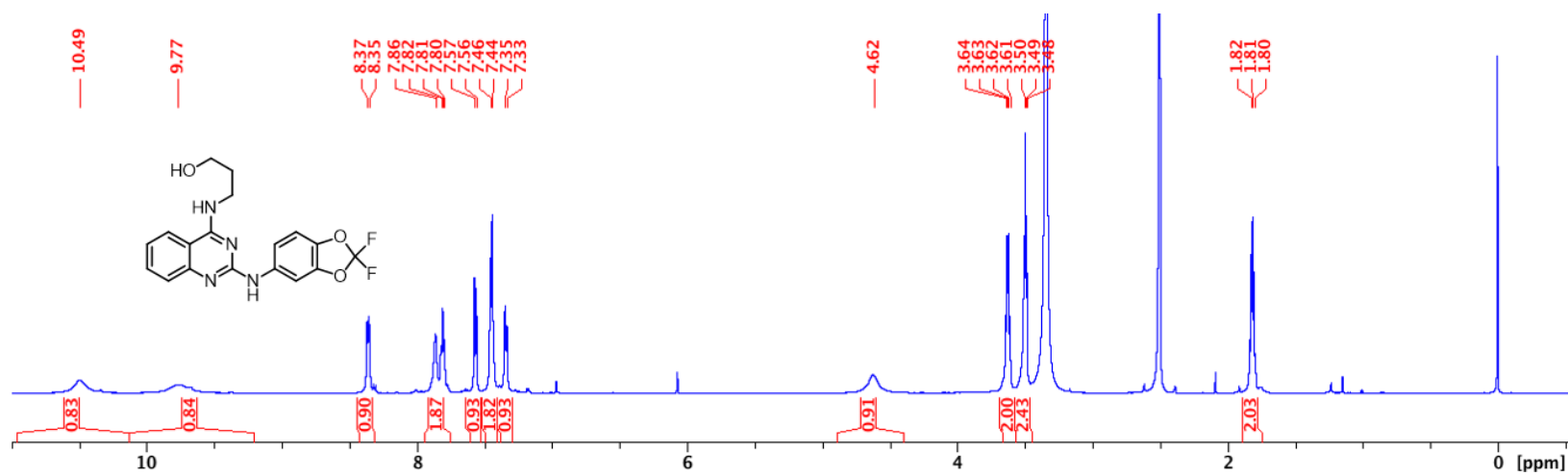




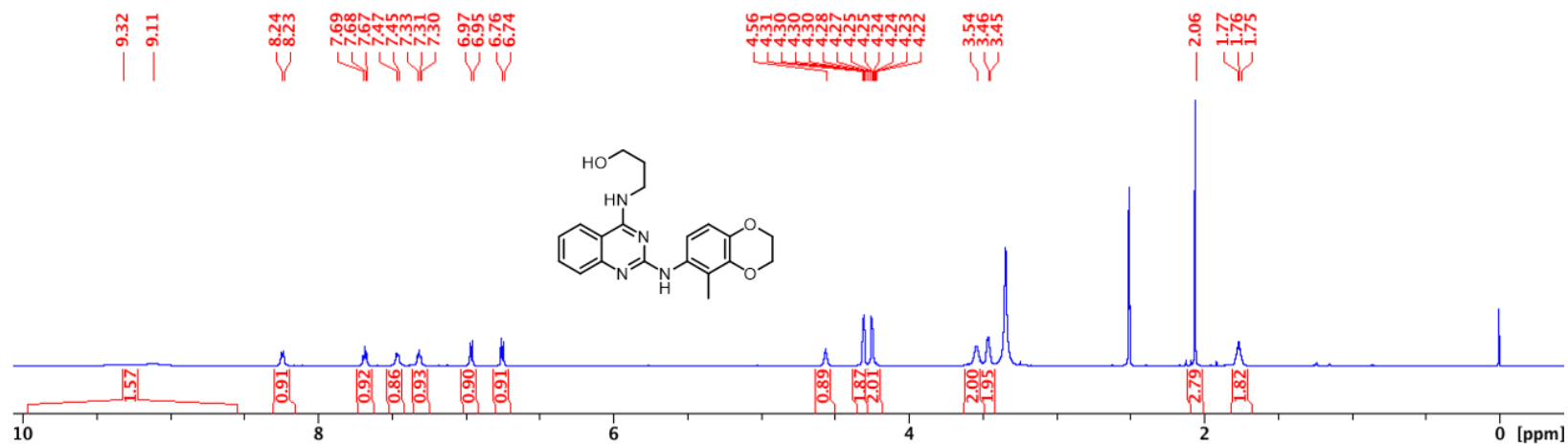
**Characterization of 45:**



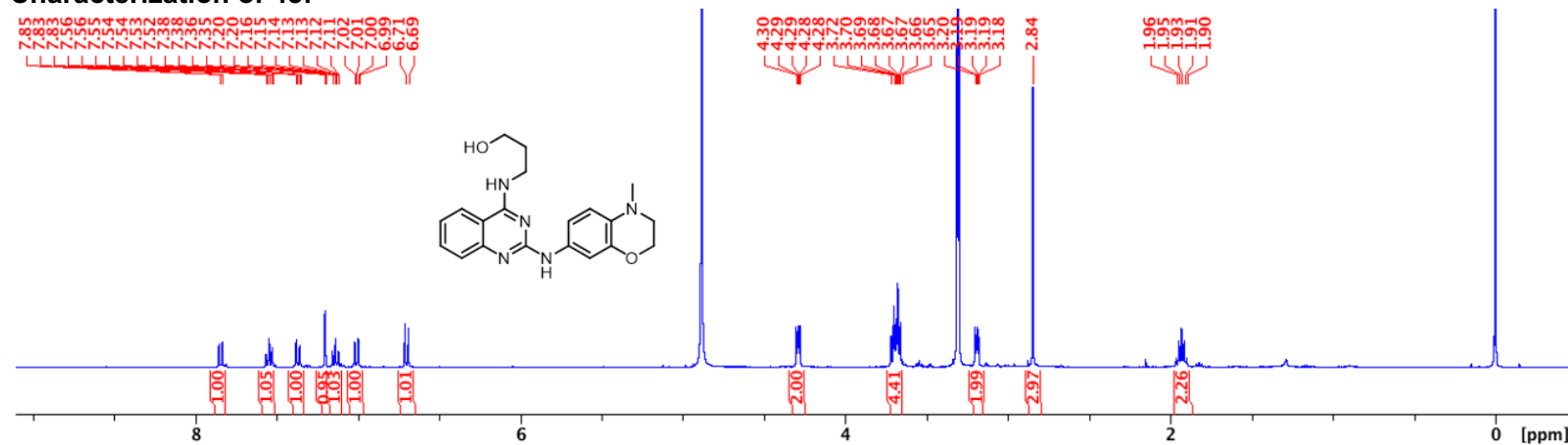
**Characterization of 46:**



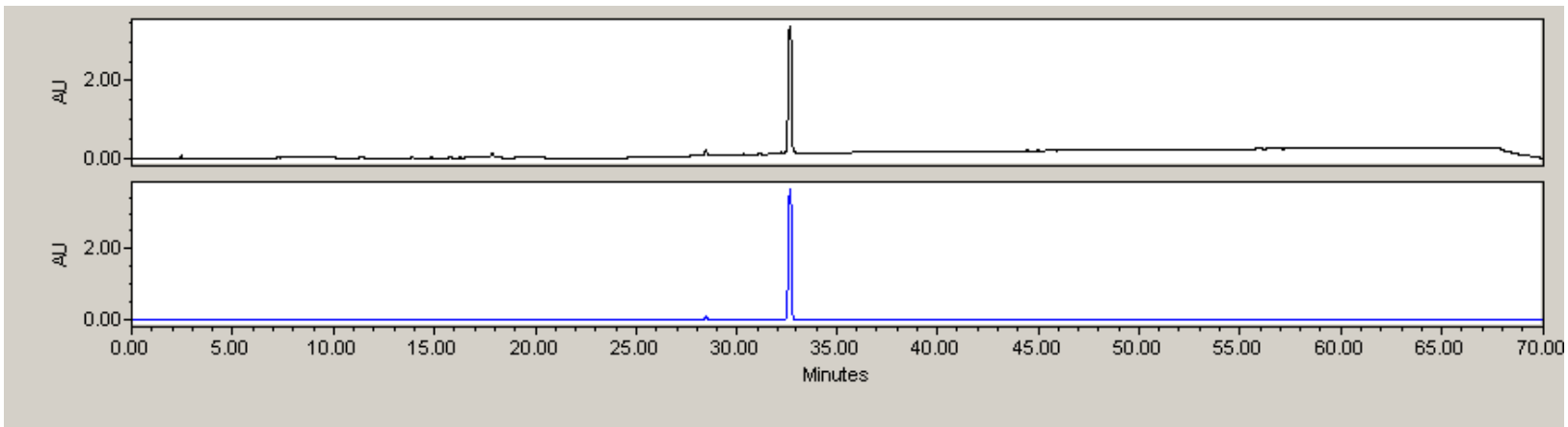
**Characterization of 47:**



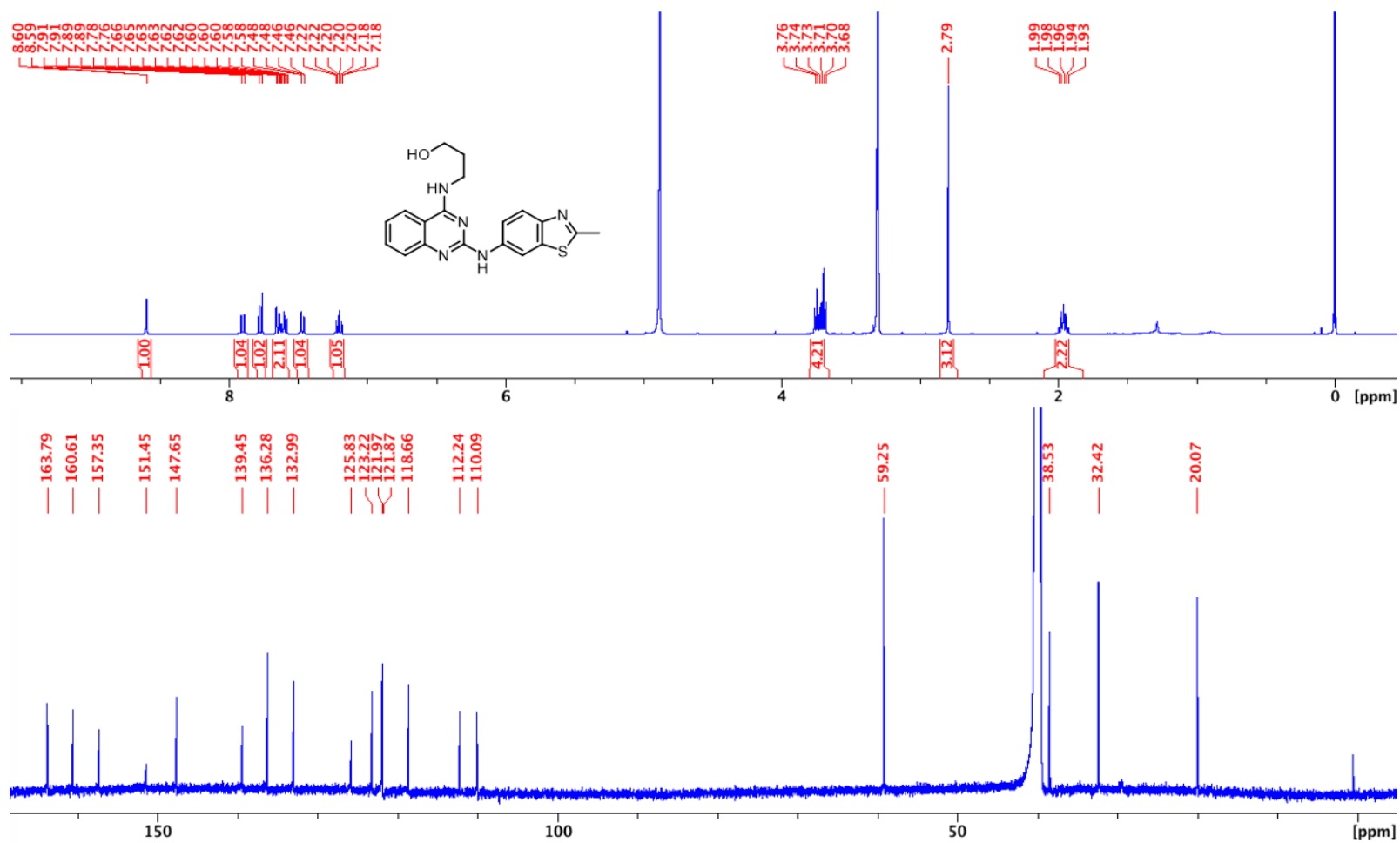
**Characterization of 48:**

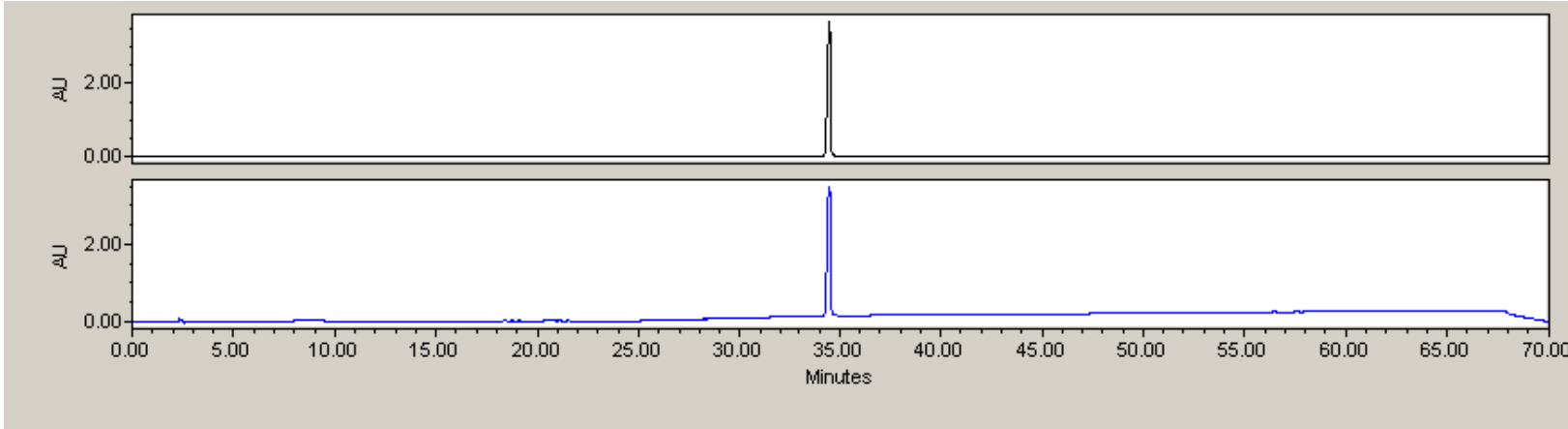




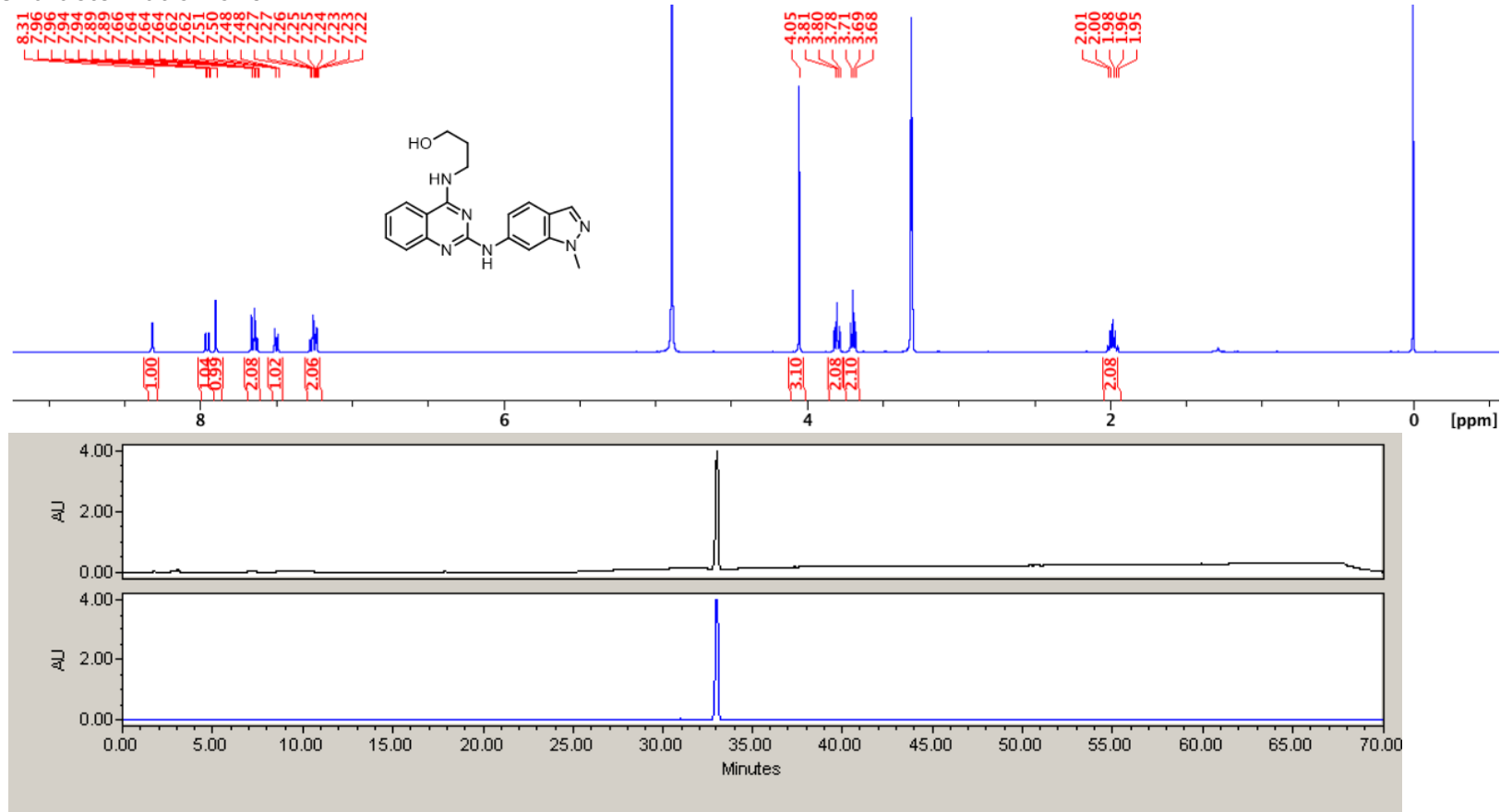


### Characterization of 50:

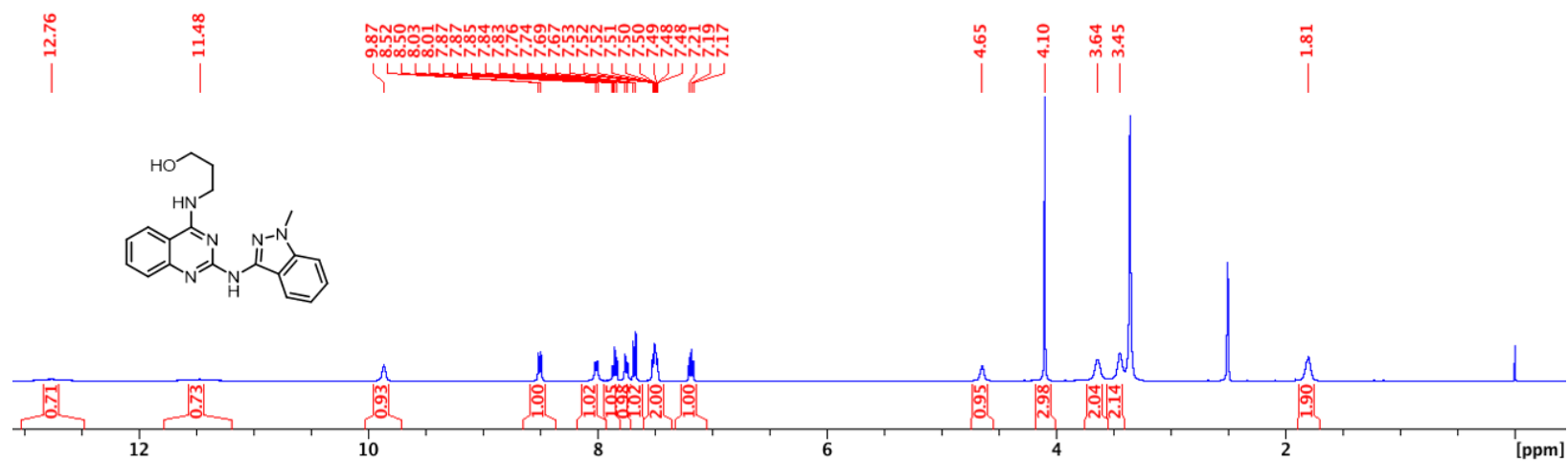




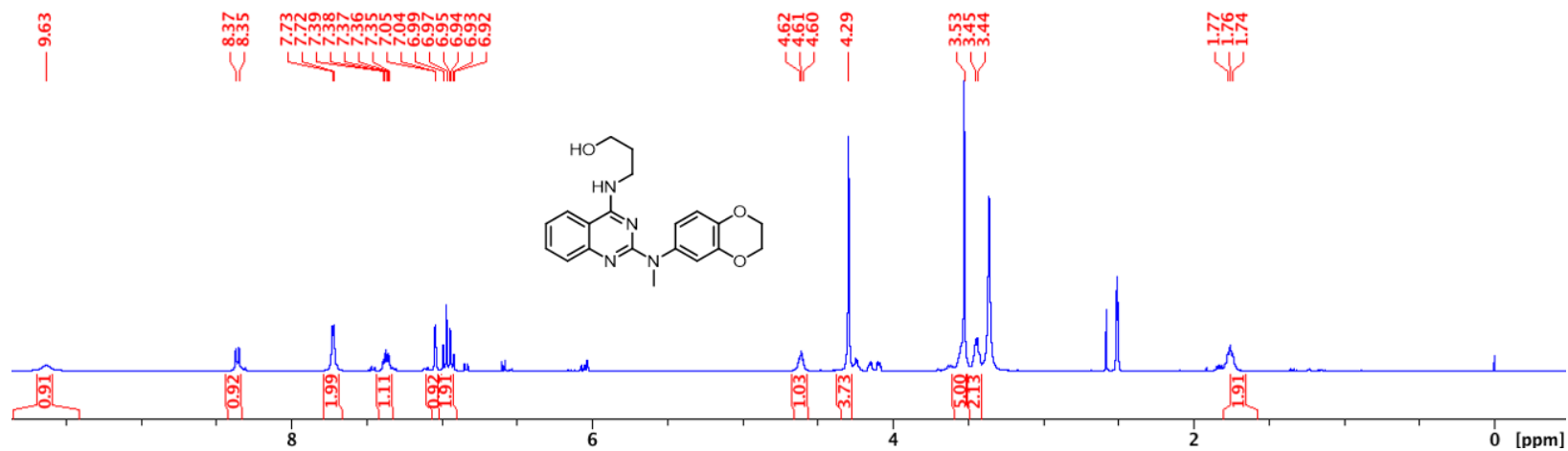
### Characterization of 51:



### Characterization of 52:



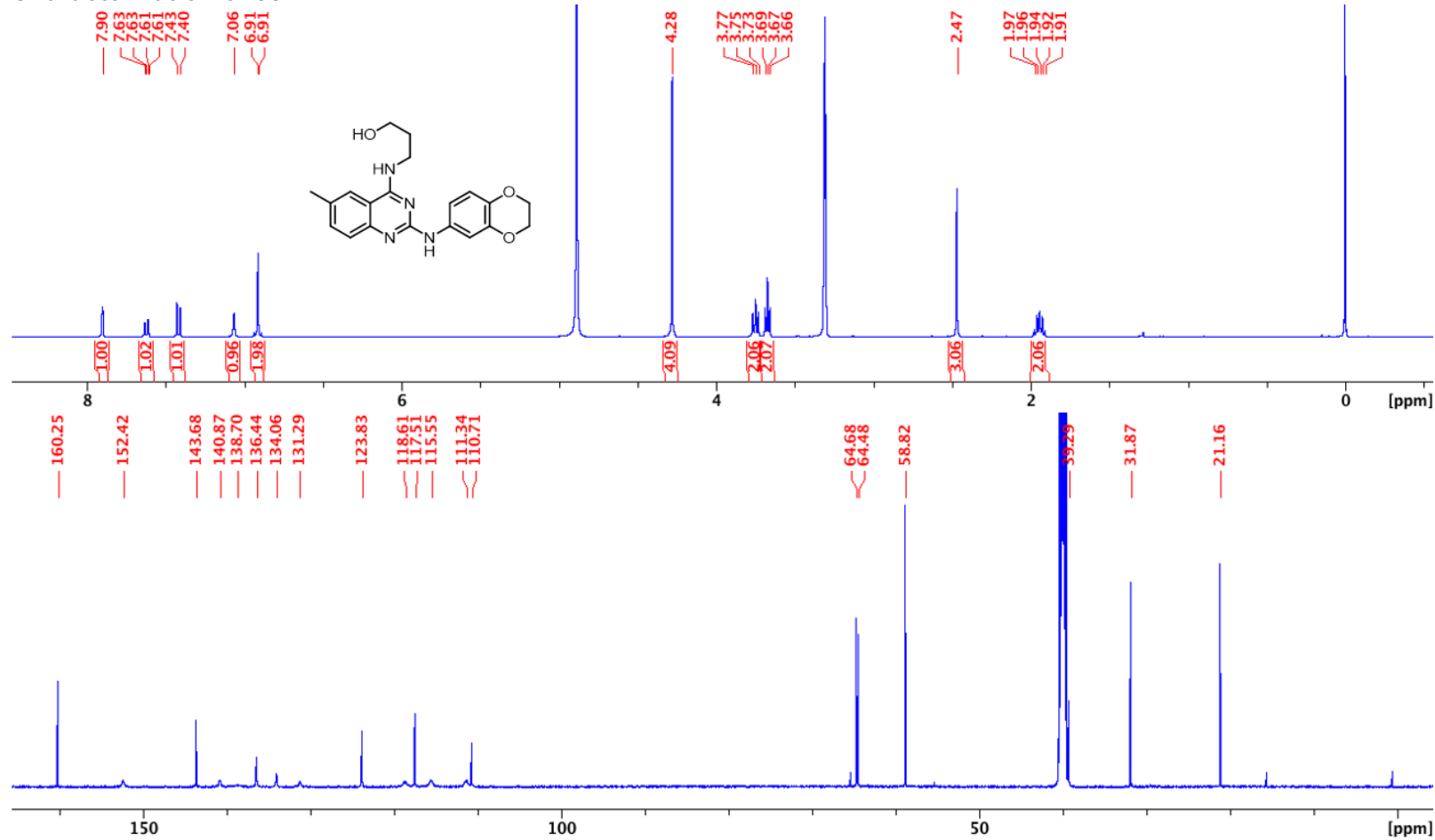
**Characterization of 53:**

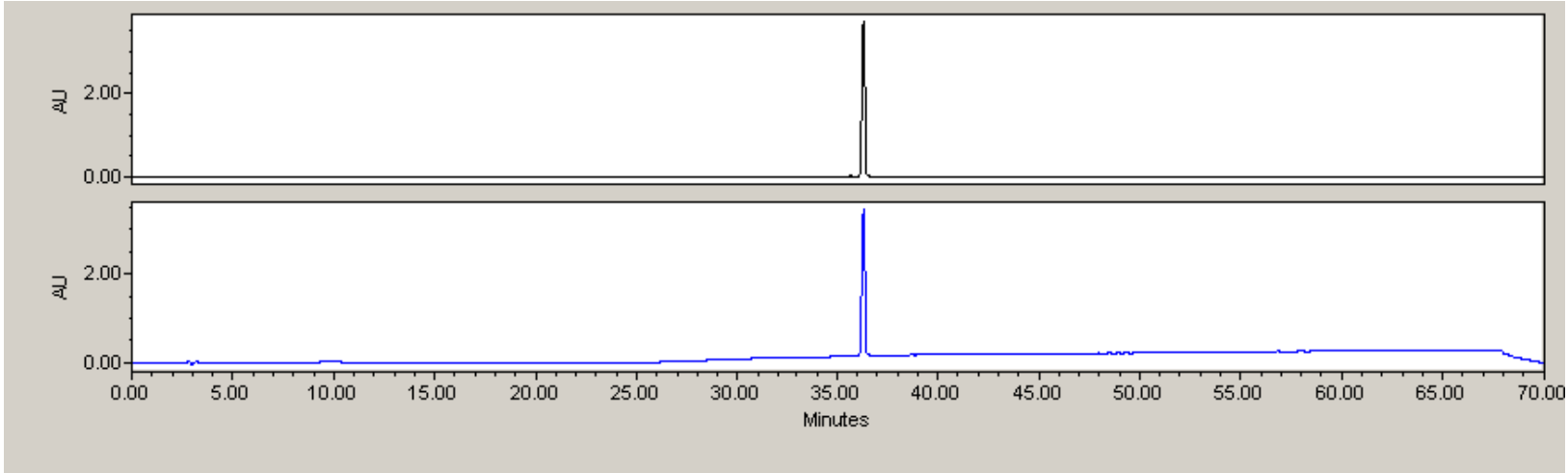




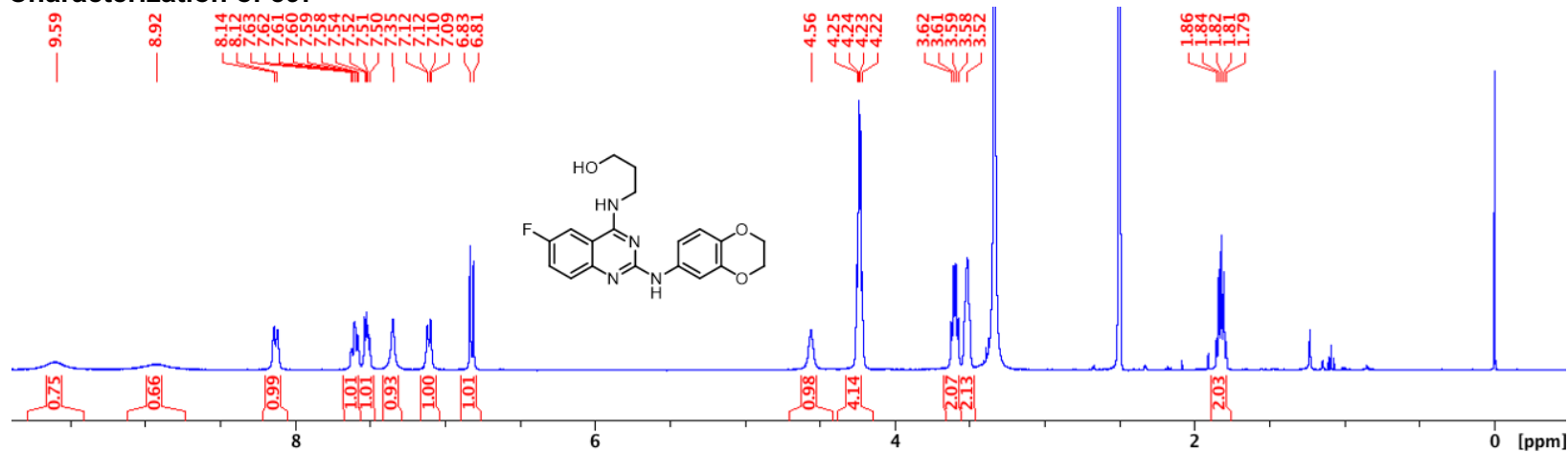


### Characterization of 58:

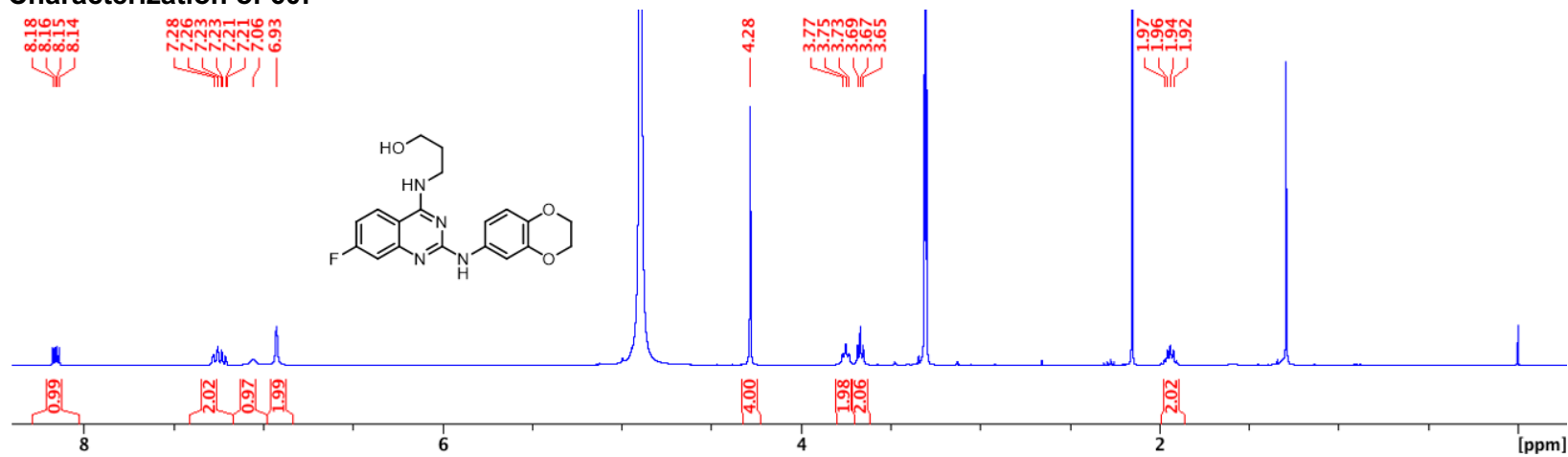




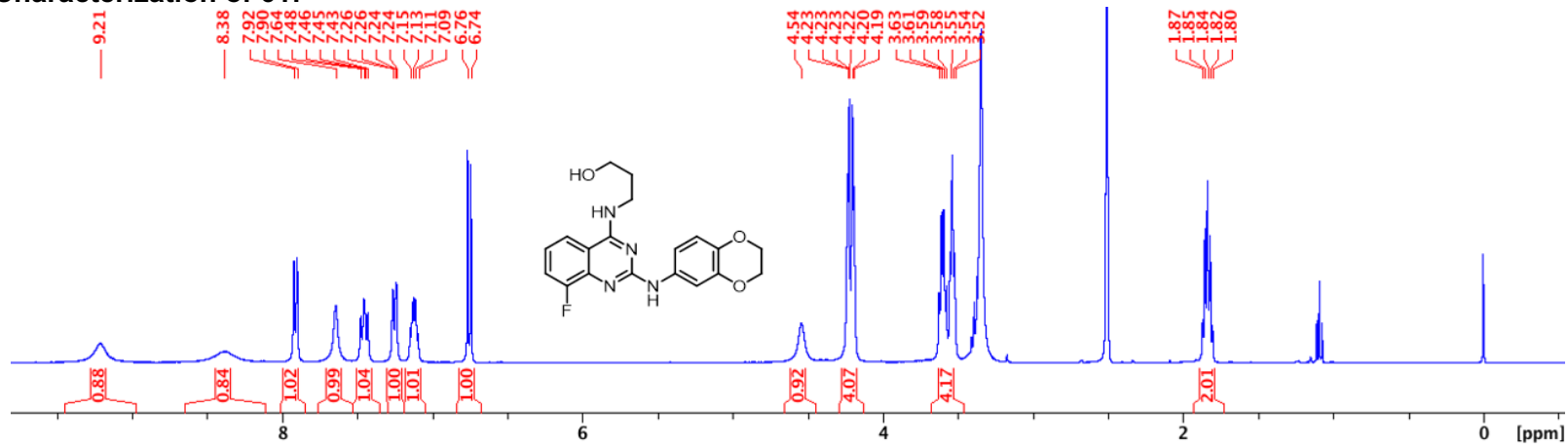
**Characterization of 59:**



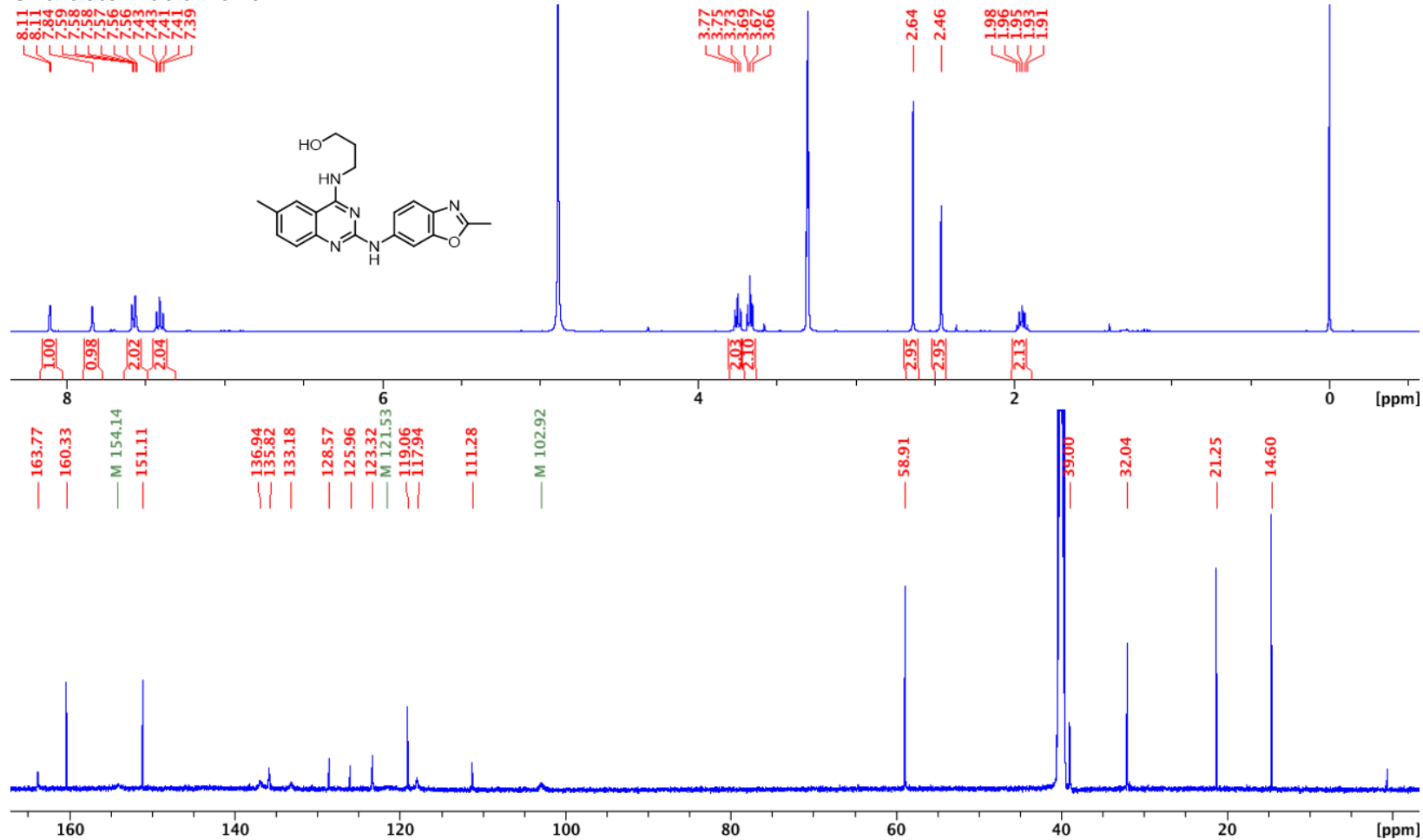
**Characterization of 60:**

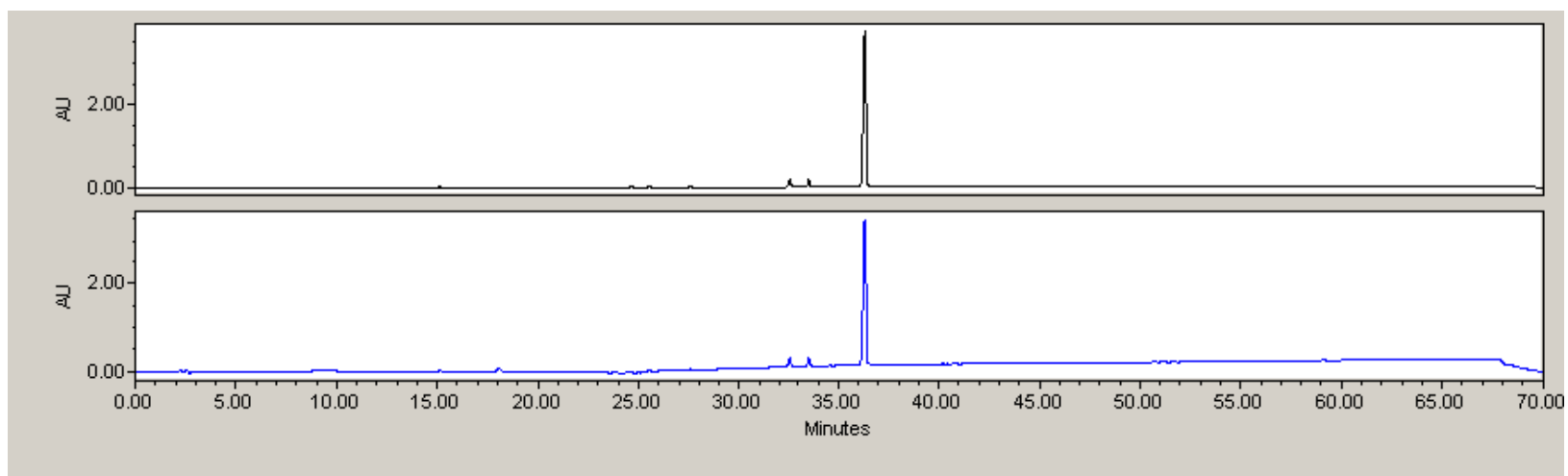


Characterization of 61:

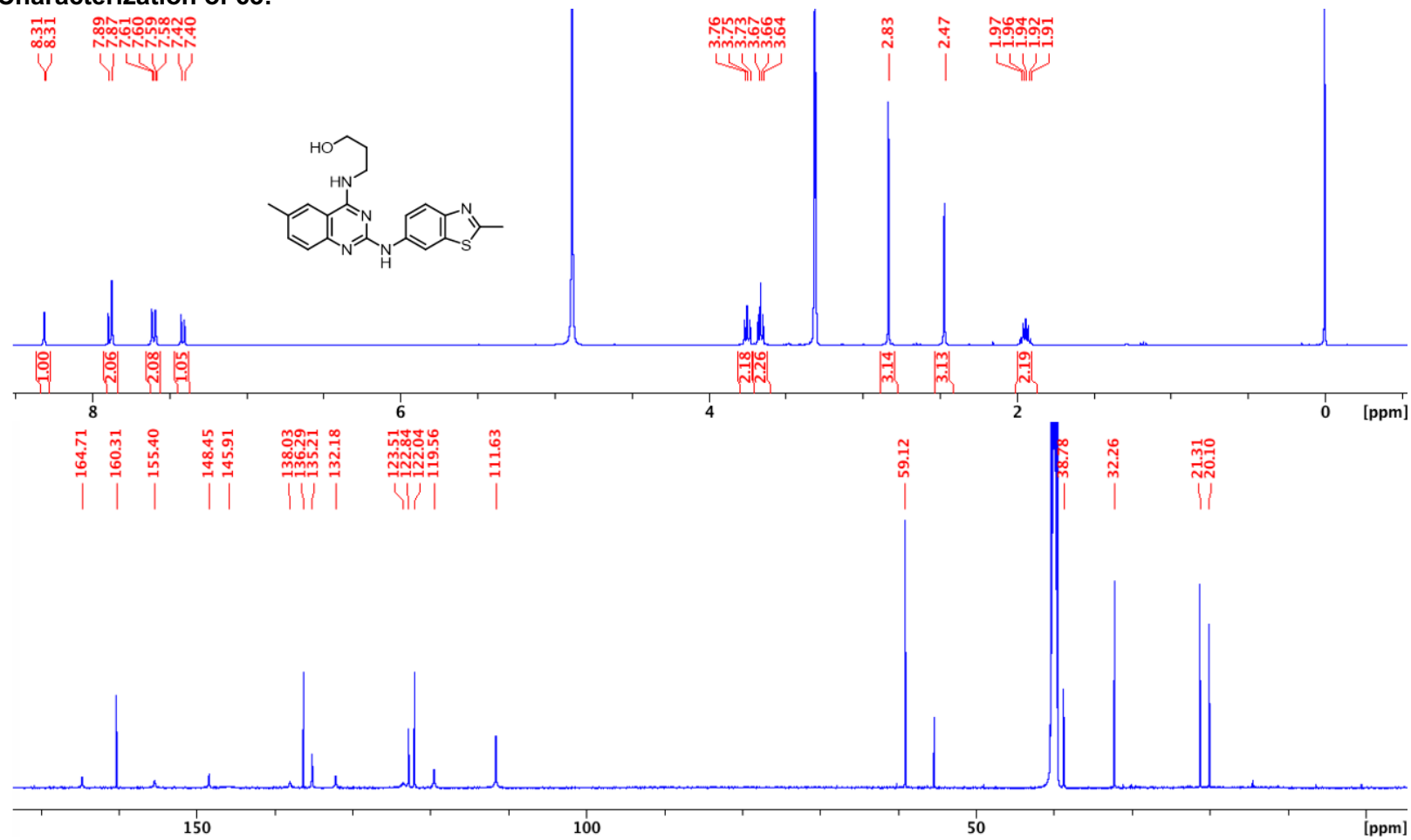


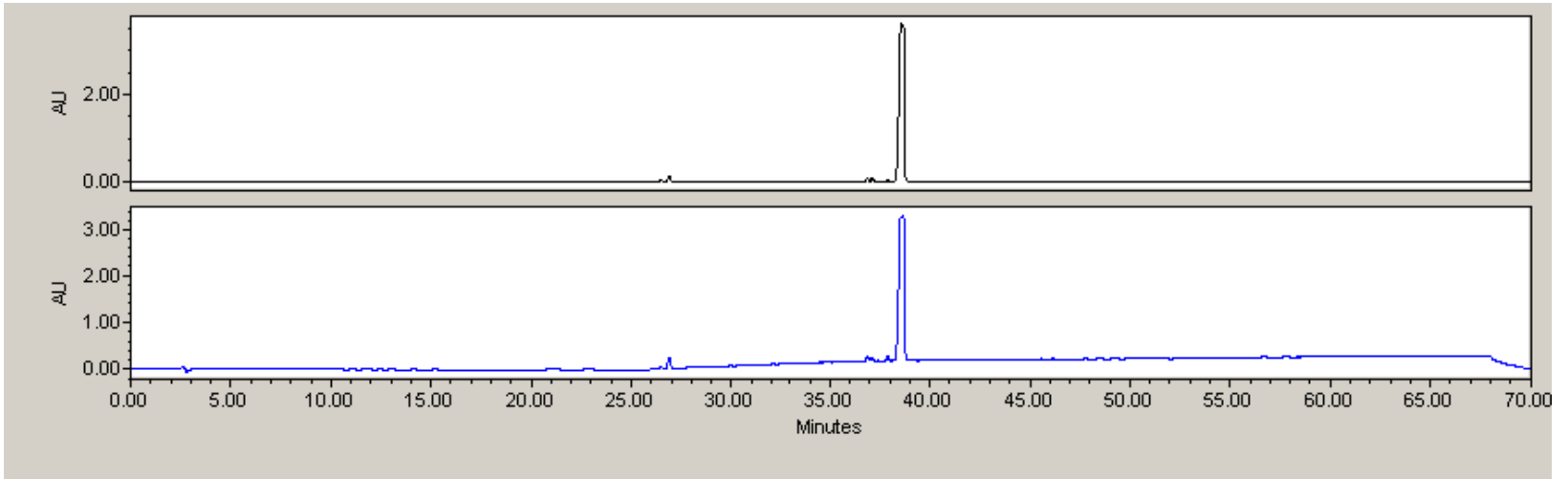
### Characterization of 62:



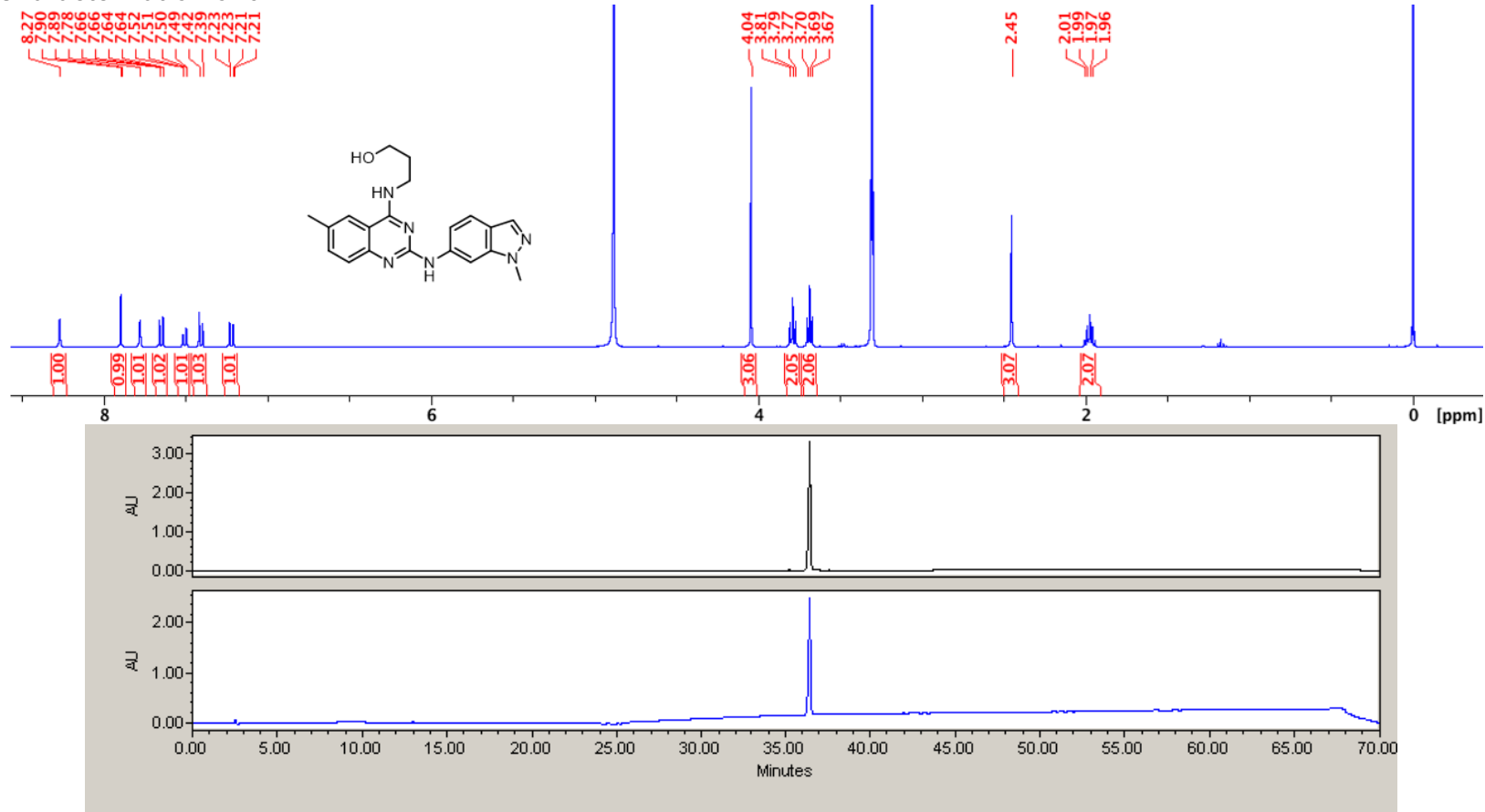


Characterization of 63:

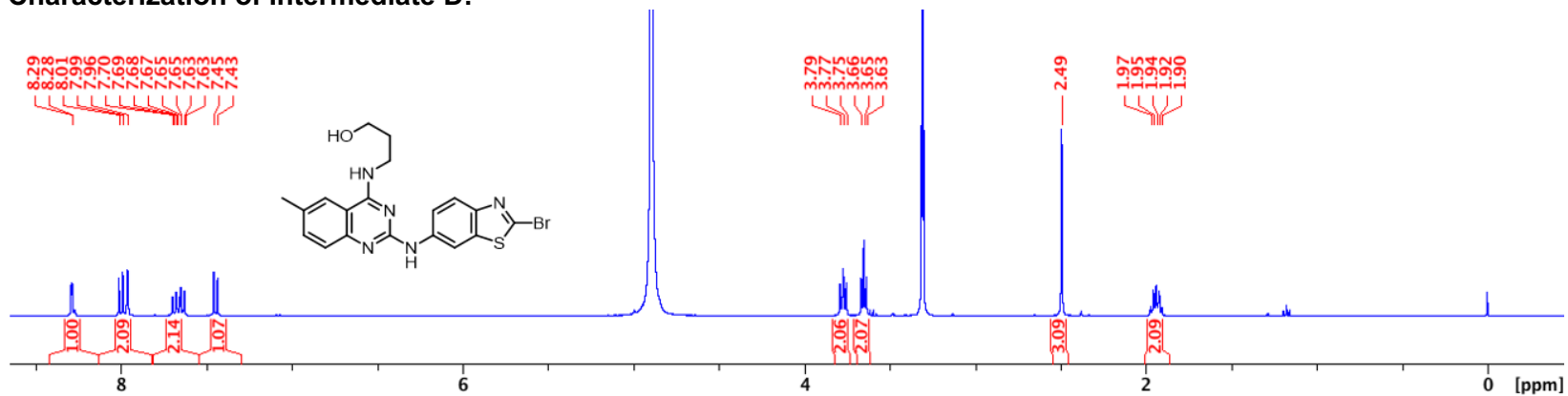




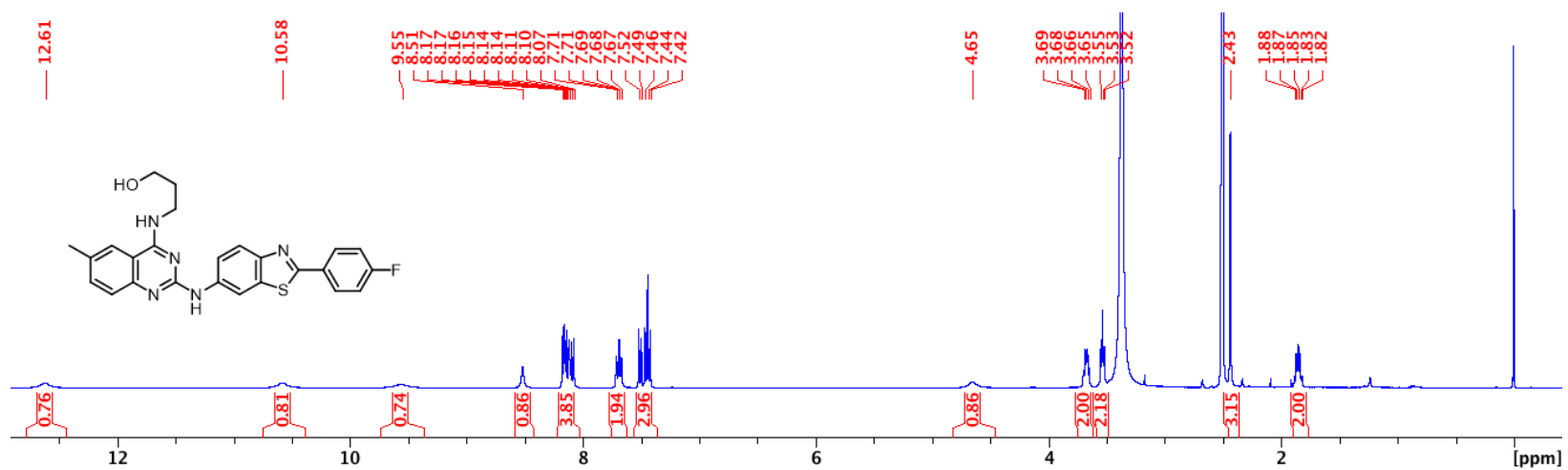
Characterization of 64:



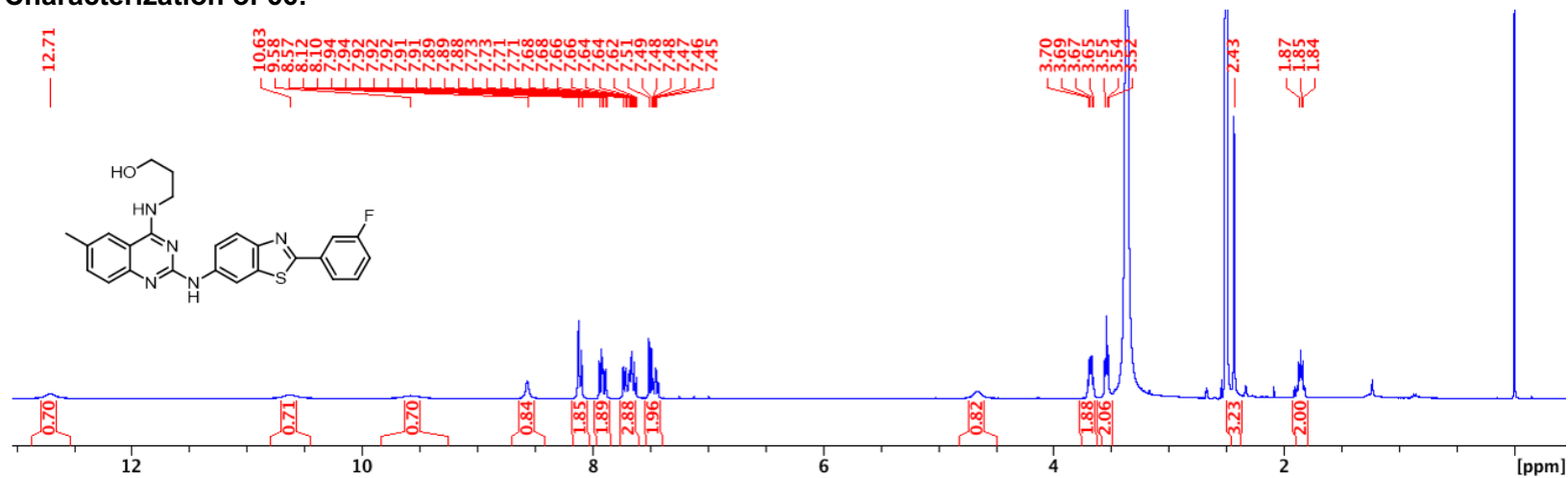
**Characterization of Intermediate D:**



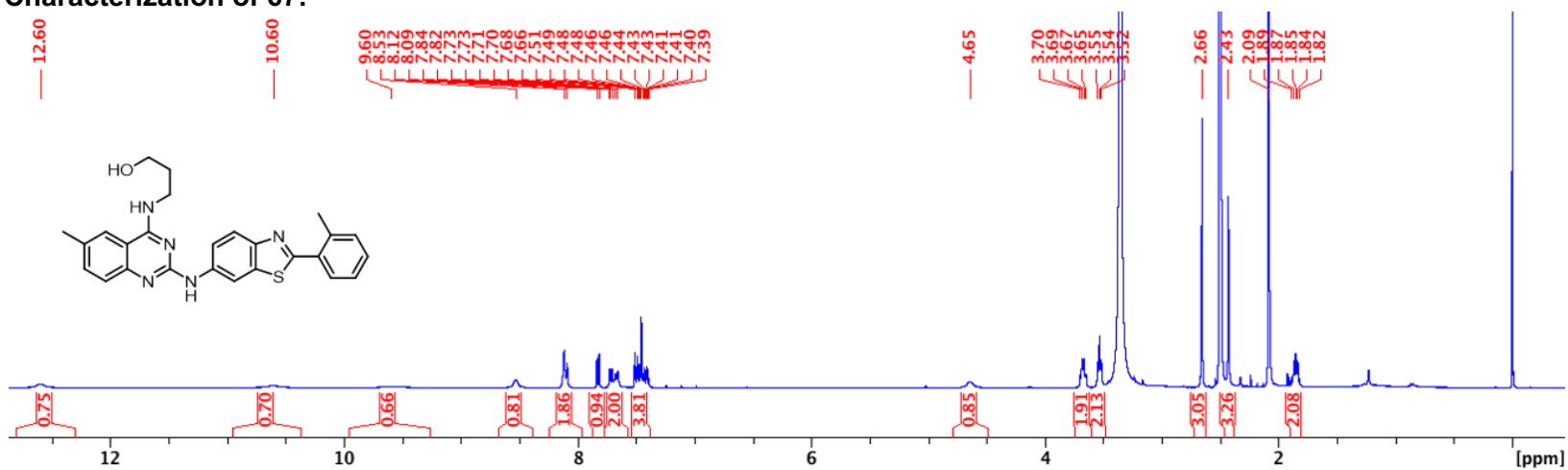
**Characterization of 65:**



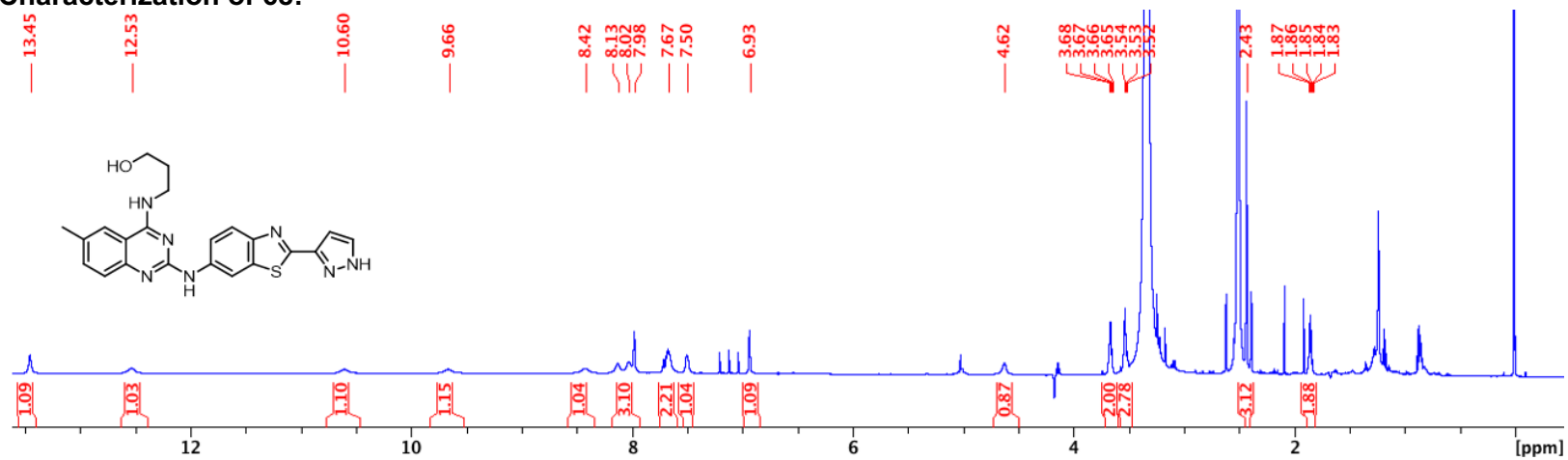
### Characterization of 66:



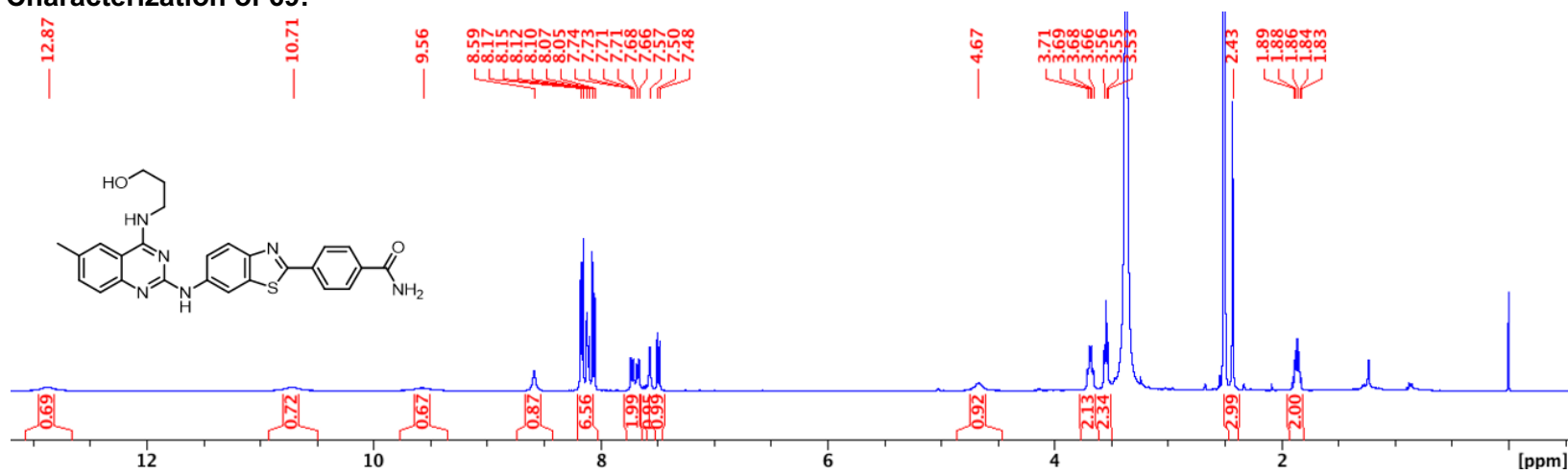
### Characterization of 67:



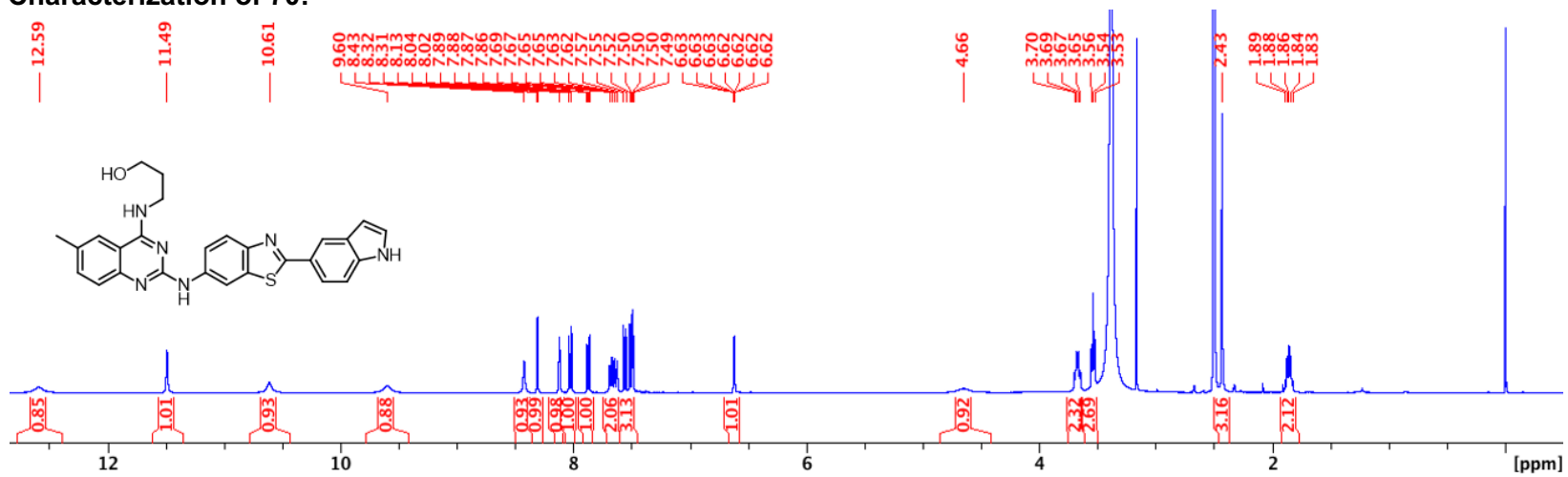
**Characterization of 68:**



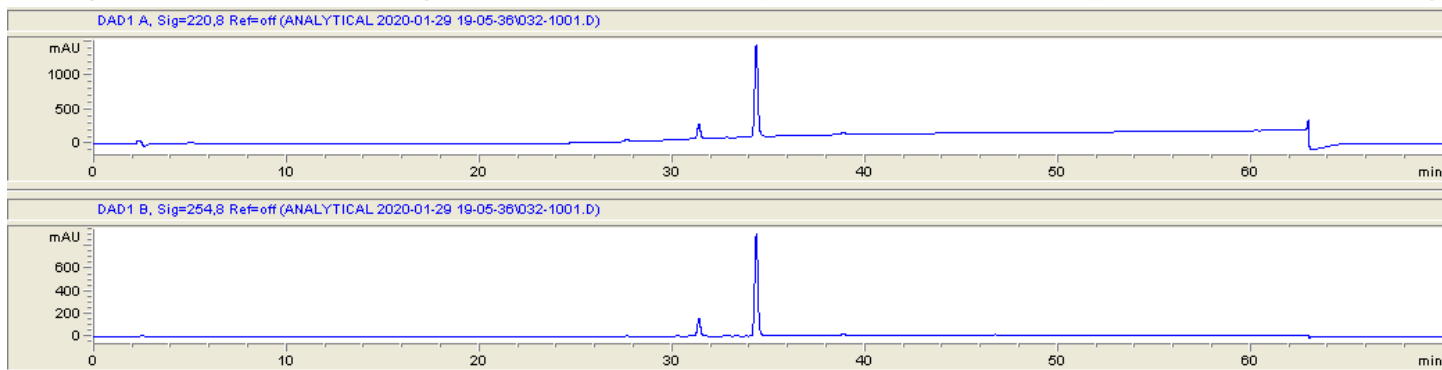
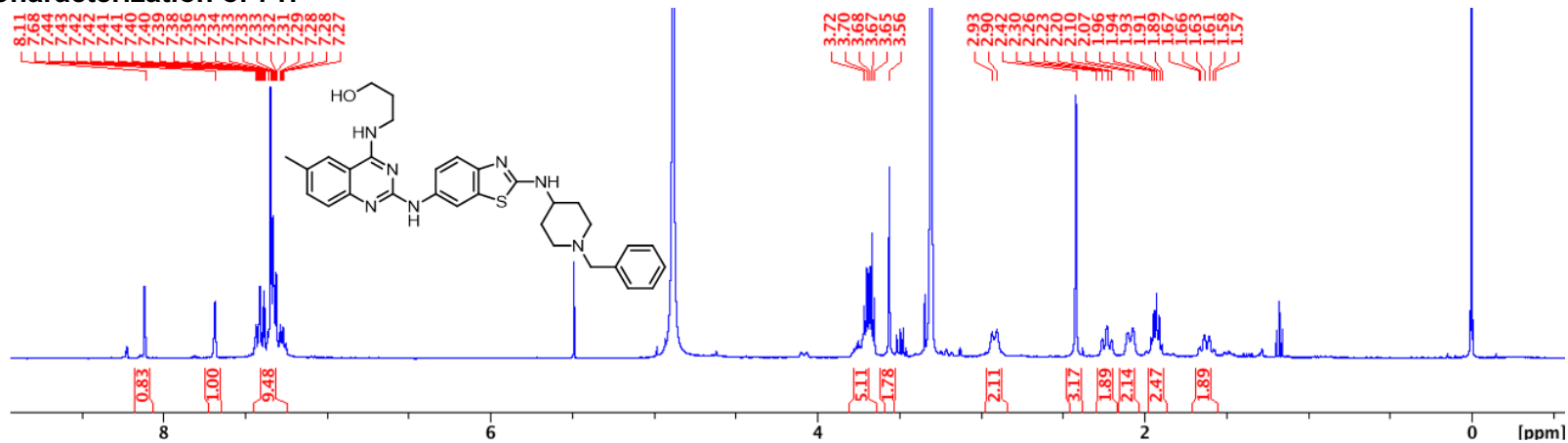
**Characterization of 69:**



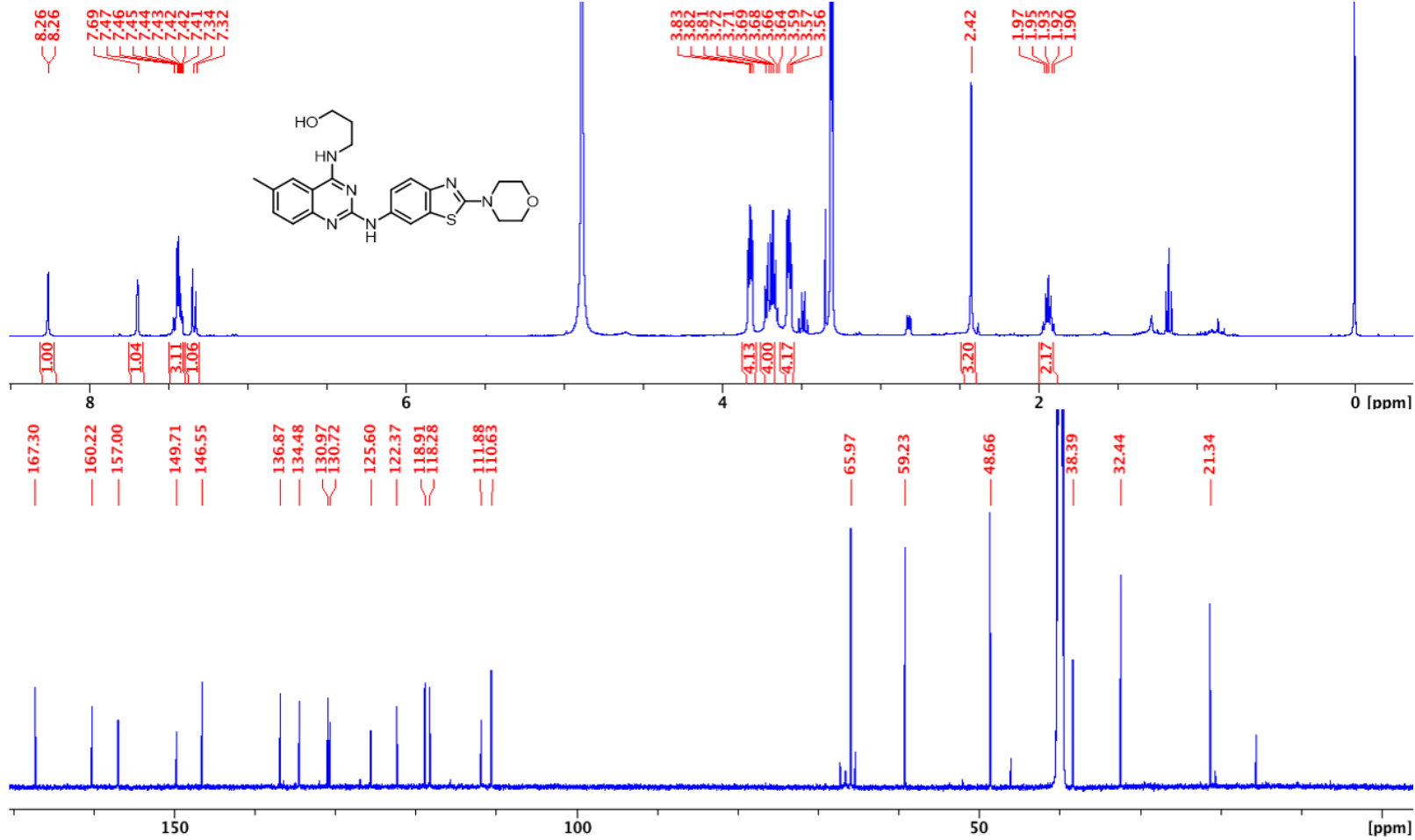
### Characterization of 70:

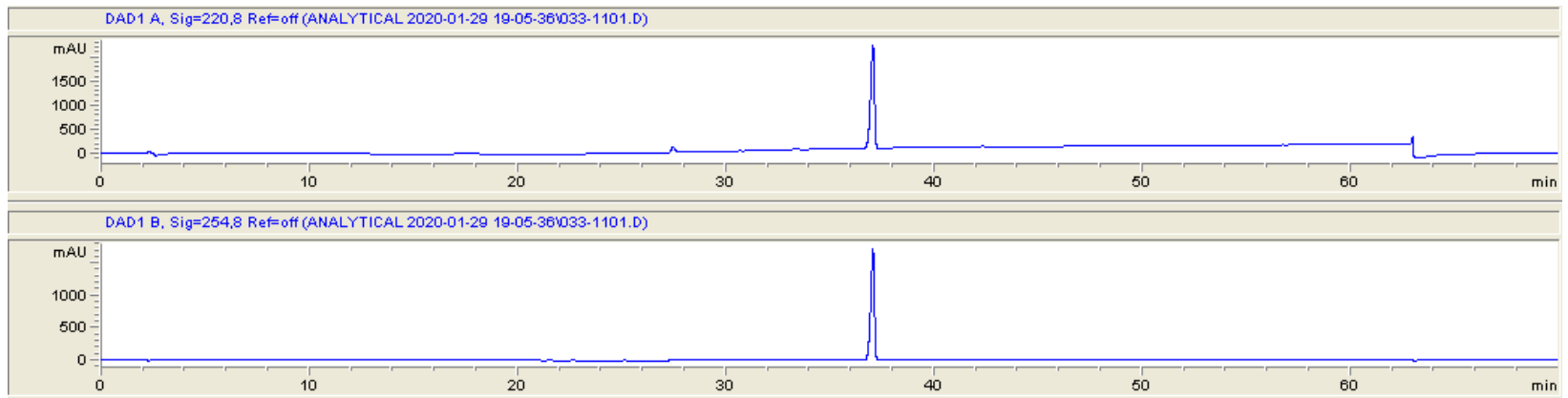


**Characterization of 71:**

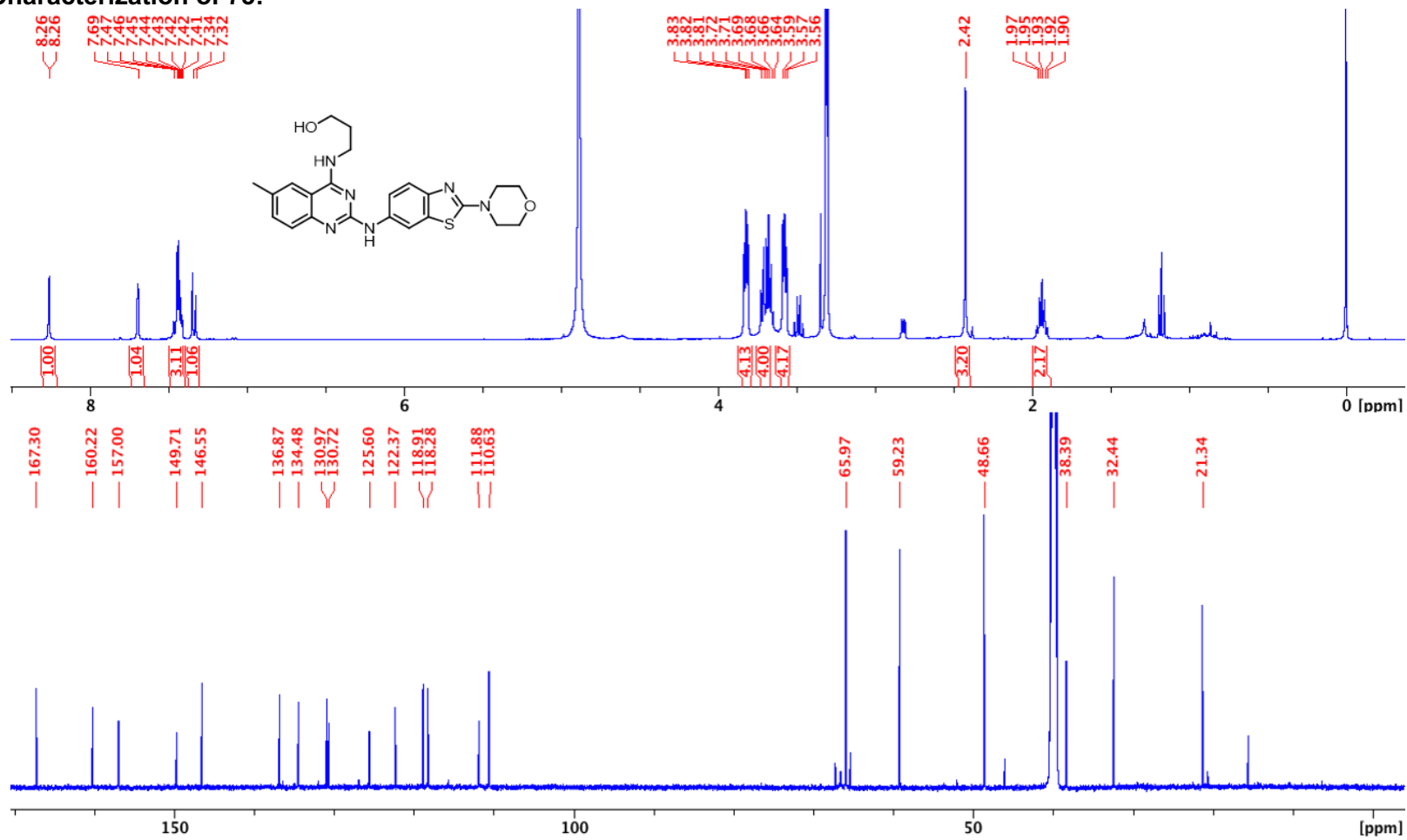


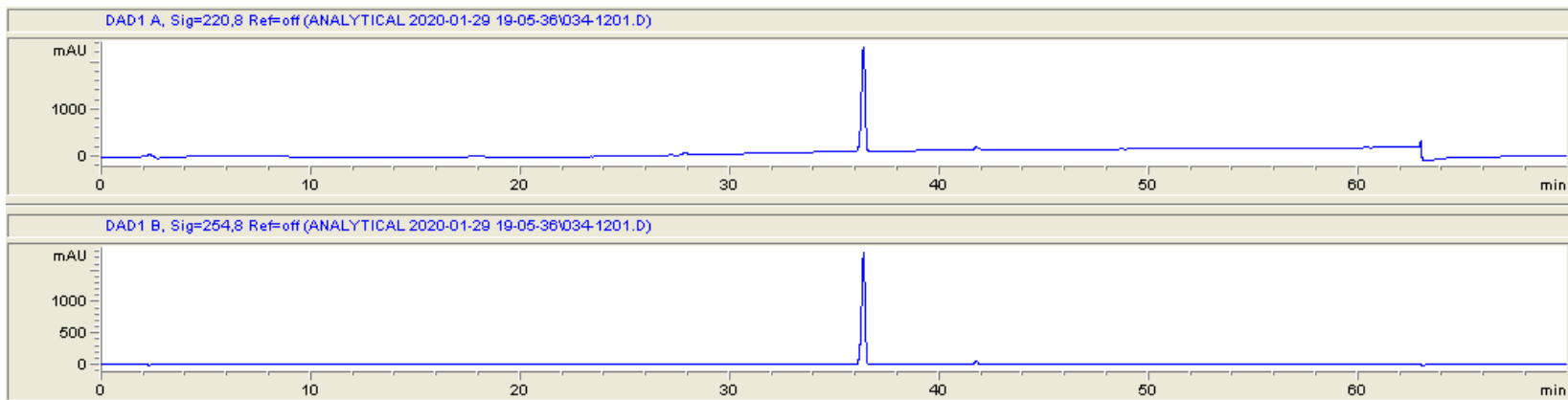
Characterization of 72:



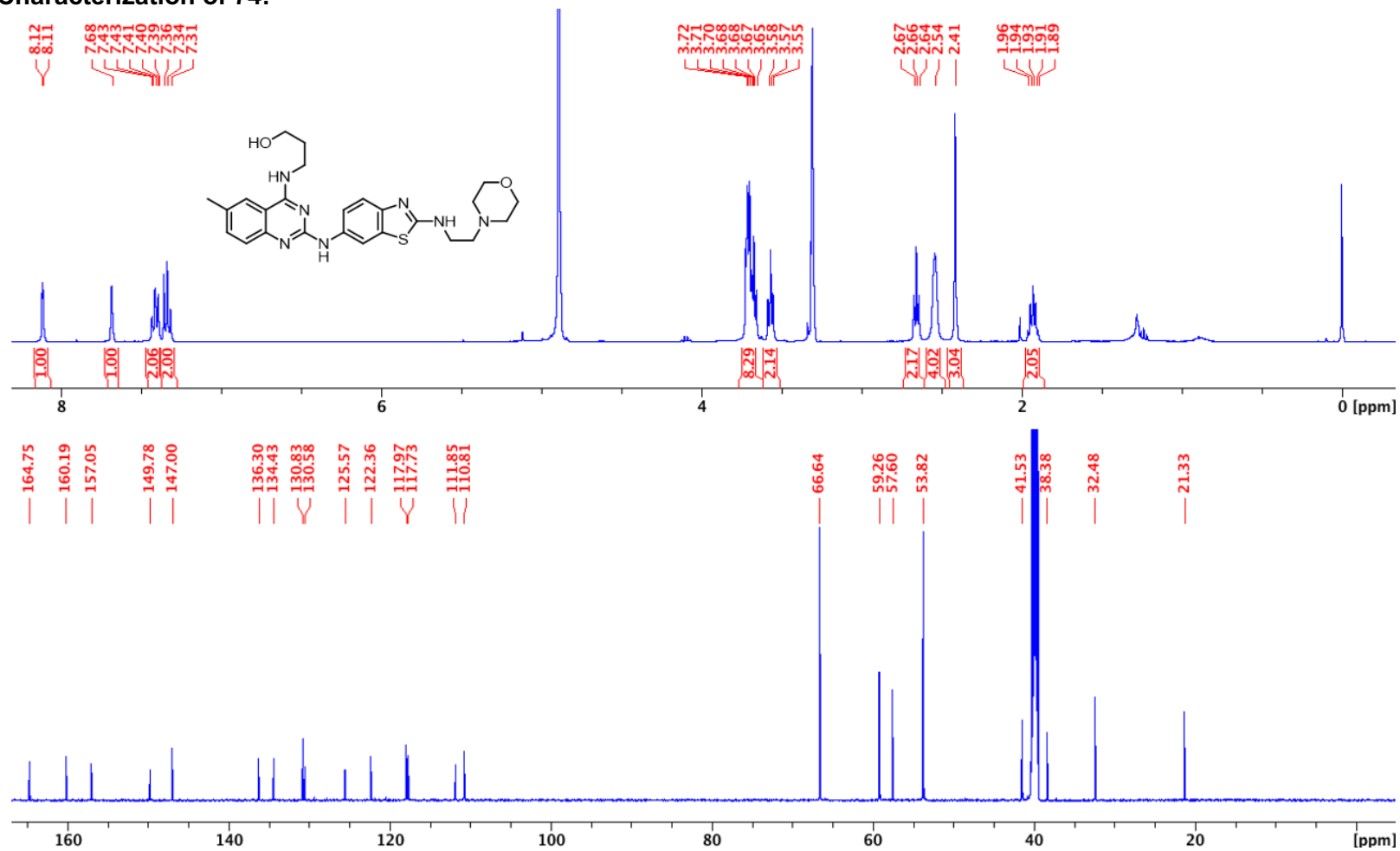


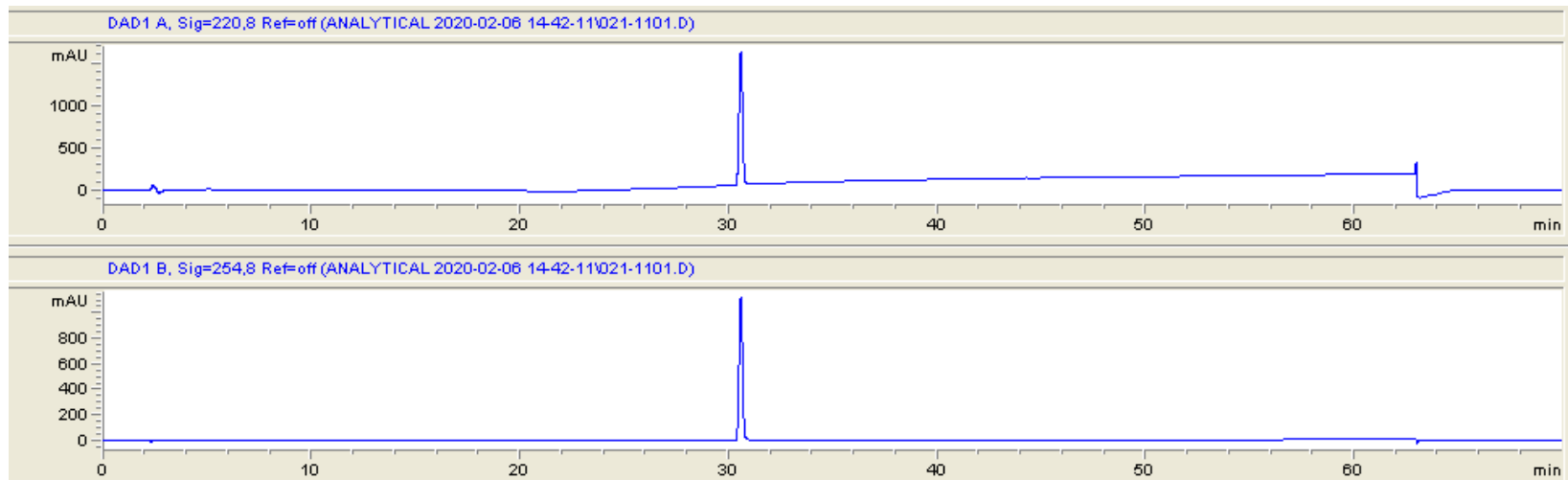
### Characterization of 73:





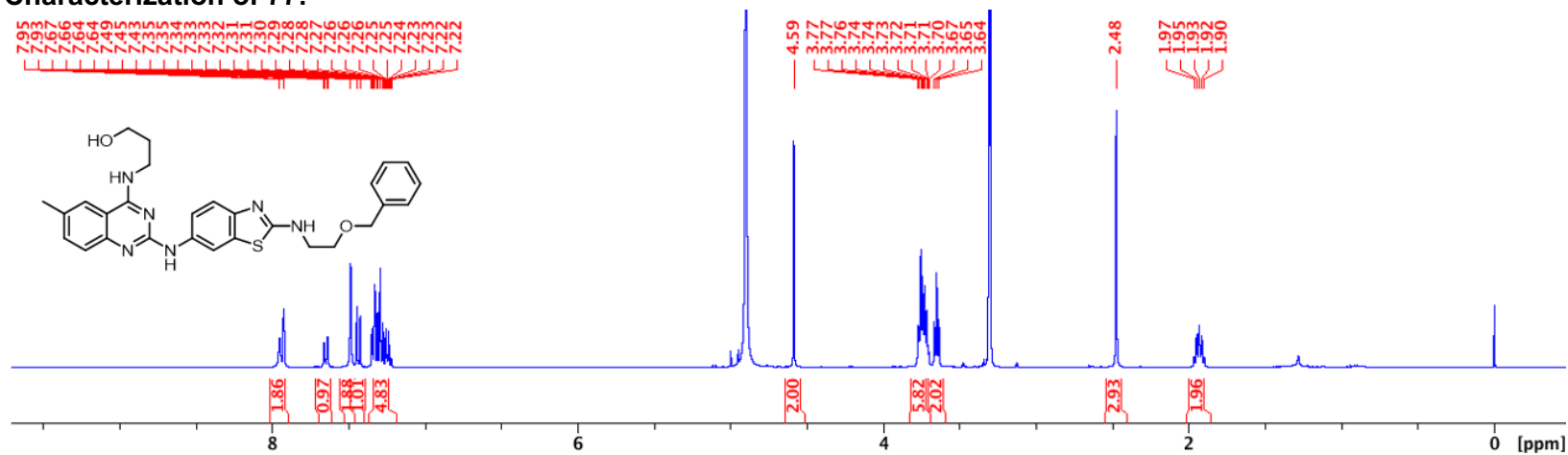
Characterization of 74:



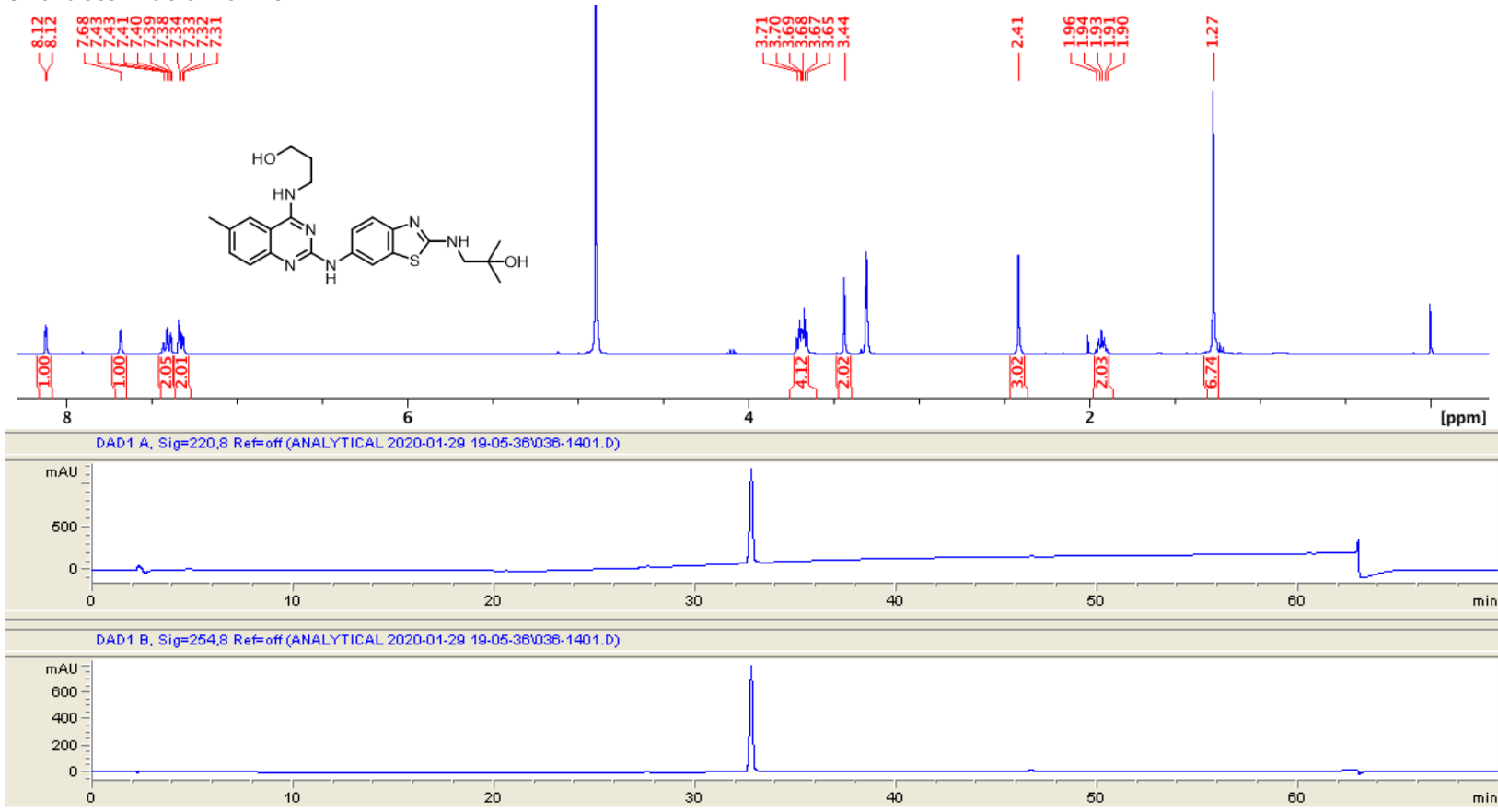




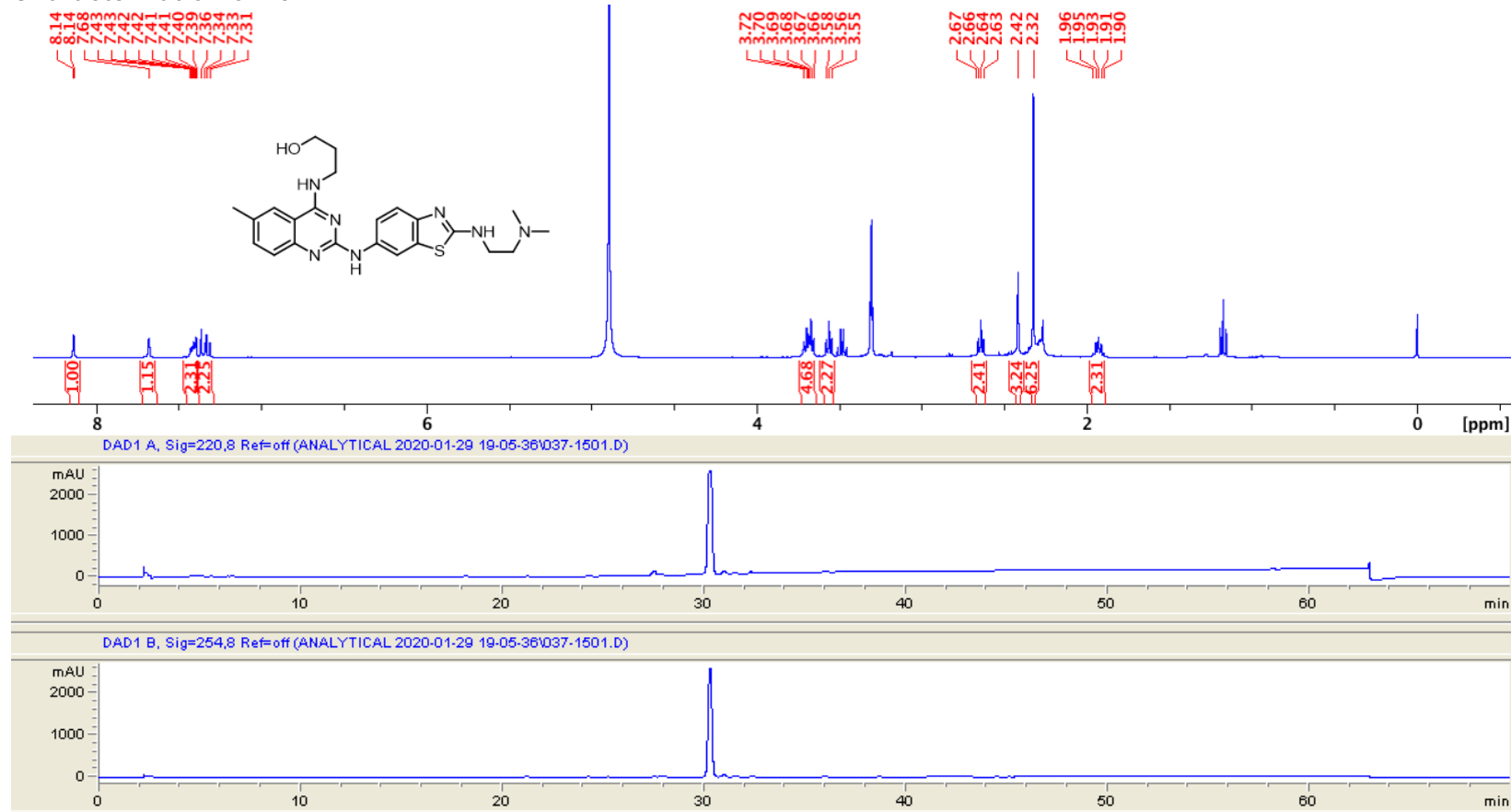
### Characterization of 77:



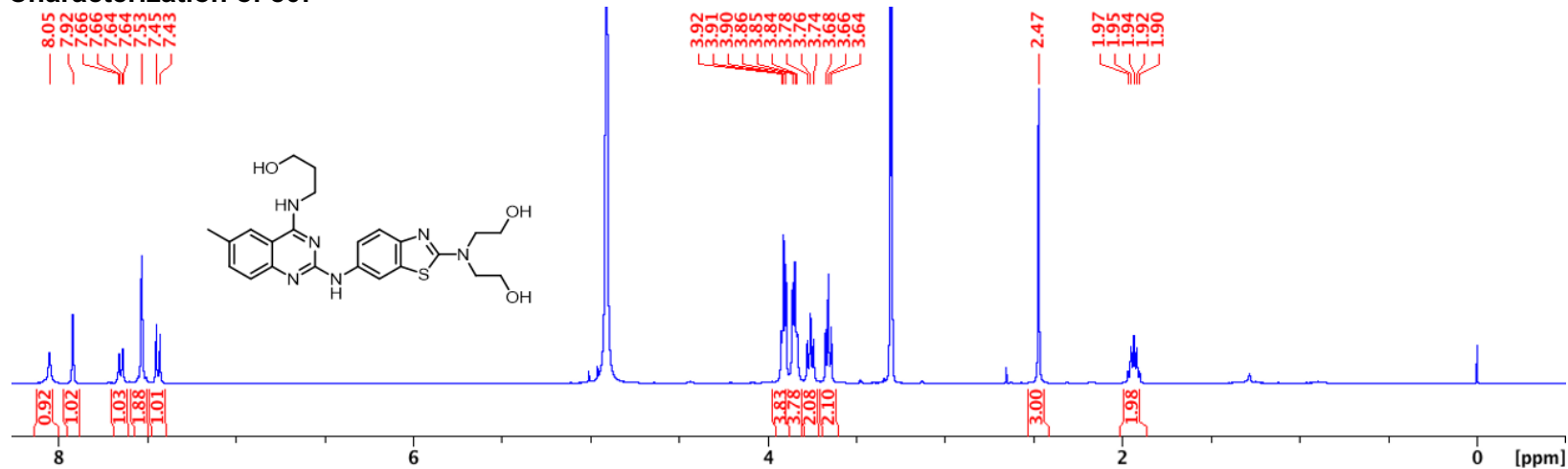
### Characterization of 78:



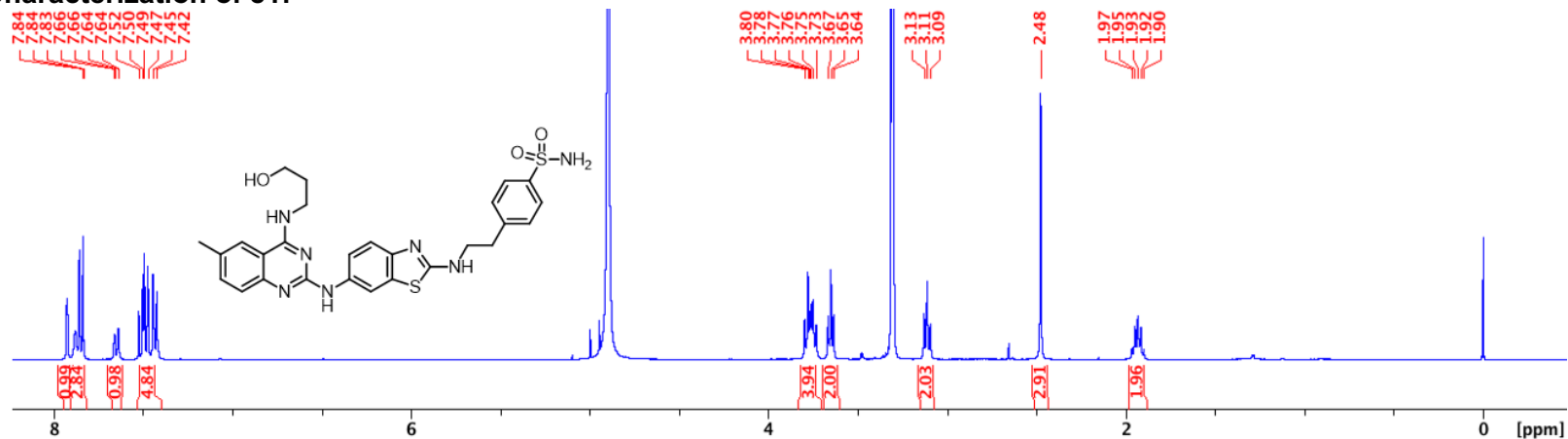
### Characterization of 79:



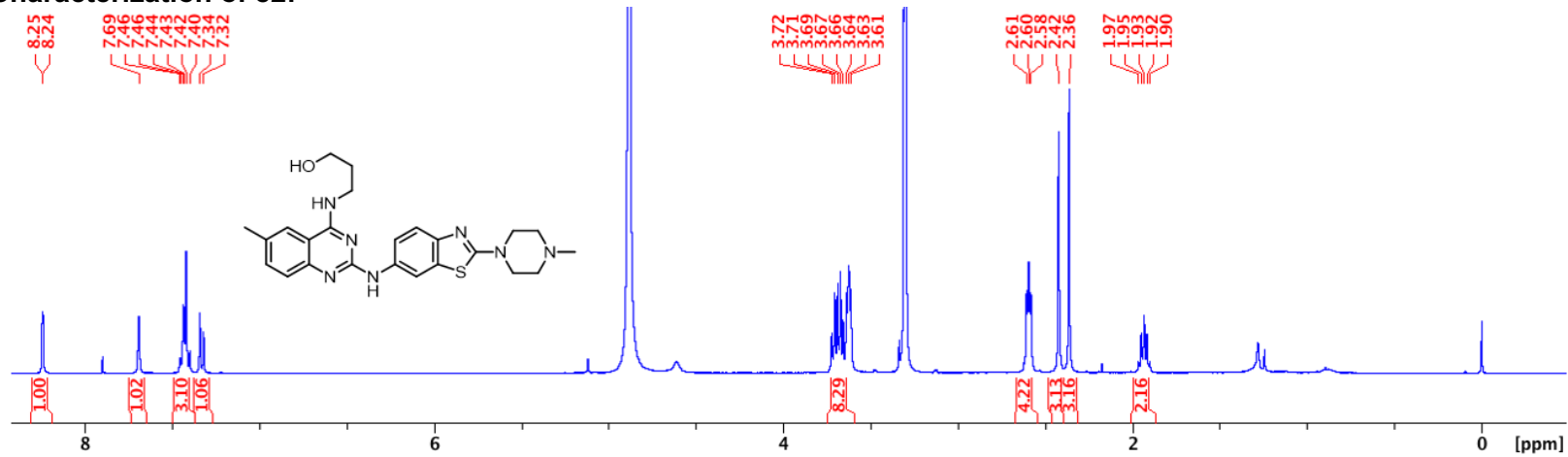
### Characterization of 80:



### Characterization of 81:



### Characterization of 82:



## REFERENCES

1. Chen, C. Z.; Sobczak, K.; Hoskins, J.; Southall, N.; Marugan, J. J.; Zheng, W.; Thornton, C. A.; Austin, C. P., Two high-throughput screening assays for aberrant RNA-protein interactions in myotonic dystrophy type 1. *Anal. Bioanal. Chem.* **2012**, *402* (5), 1889-98.